REMOVAL OF *N*-NITROSAMINES BY NANOFILTRATION AND REVERSE OSMOSIS MEMBRANES

A Thesis
Presented to
The Academic Faculty

By

Yu Miyashita

In Partial Fulfillment
Of the Requirements for the Degree
Master of Science in Environmental Engineering

Georgia Institute of Technology

May 2007

REMOVAL OF *N*-NITROSAMINES
BY NANOFILTRATION AND REVERSE OSMOSIS MEMBRANES

Approved By:

Dr. Jae-hong Kim
School of Civil and Environmental Engineering
Georgia Institute of Technology

Dr. Ching-Hua Huang
School of Civil and Environmental Engineering
Georgia Institute of Technology

Dr. Sotira Yiacoumi
School of Civil and Environmental Engineering
Georgia Institute of Technology

Date Approved: April 6, 2007

ACKNOWLEDGMENTS

I would like to acknowledge Saehan Industries Inc. for providing financial support and membrane samples for this project and Dow Chemical Company is also thanked for providing membrane samples for testing. Dr. Jae-Hong Kim provided great guidance and encouragement throughout the project. I would especially like to thank my committee members, Dr. Ching-Hua Huang and Dr. Sotira Yiacoumi, for spending time and effort to review this thesis. I gratefully acknowledge Joo-Yeon Lee, Hoon Hyung and Amisha Shah for assistance and advice in conducting experiments, Sang-Hyuck Park and Lokesh Padhye for significant assistance in nitrosamine analyses and Dooil Kim, Pranay Mane and Wan-Ru Chen for helpful suggestions.

TABLE OF CONTENTS

LIST OF TABLES

LIST OF FIGURES

LIST OF ABBREVIATIONS

AC	Activated carbon
CV	Coefficient of variation
DBA	Disinfection by-products
DMA	Dimethylamine
EDCs	Endocrine disrupting chemicals
EPA	Environmental Protection Agency
GAC	Granular activated carbon
GC/MS	Gas chromatography/mass spectrometry
GPM	Gallon per minute
HPLC	High performance liquid chromatography
LLE	Liquid-liquid extraction
LMH	Liter per square meter per hour
LVI	Large volume injector
NA	Nitrosamine
NDBA	*N*- nitrosodi-n-butylamine
NDEA	*N*-nitrosodiethylamine
NDMA	*N*-nitrosodimethylamine
NDPA	*N*-nitrosodi-n-propylamine
NDPHA	*N*-nitrosodiphenylamine
NF	Nanofiltration
NMEA	*N*-nitrosomethylethylamine
NPYR	*N*-nitrosopyrrolidine
PhAcs	Pharmaceutically active compounds
PTV	Programmable temperature vaporization
RO	Reverse osmosis
SIM	Selected ion monitoring
SPE	Solid-phase extraction

SUMMARY

The rejections of selected *N*-nitrosamines by commonly used high-pressure nanofiltration (NF) and reverse osmosis (RO) membranes were quantitatively evaluated using a bench-scale cross-flow filtration apparatus. The selected nitrosamines included *N*-nitrosodimethylamine (NDMA), *N*-nitrosomethylethylamine (NMEA), *N*-nitrosopyrrolidine (NPYR), *N*-nitrosodiethylamine (NDEA), *N*-nitrosodi-n-propylamine (NDPA), *N*-nitrosodi-n-butylamine (NDBA) and *N*-nitrosodiphenylamine (NDPHA). Nitrosamine rejections were evaluated under steady state at elevated feed concentrations, since NDMA rejections were found to be consistent with feed concentrations over three orders of magnitude. The steady-state nitrosamine rejections by NF membranes varied significantly, from 9 to 75%, depending on nitrosamine compounds and tested membranes. For hydrophilic compounds, rejections increased with increasing molecular weight. The nitrosamine rejections by brackish RO membranes reached as high as 97% for higher molecular weight nitrosamines. However, for low molecular weight nitrosamines such as NDMA, rejections as low as 54% were observed. This low level of rejections was attributed to diffusive solute transport being more effective than convective transport. Physicochemical properties such as molecular weight and aqueous diffusivity showed reasonable correlations with nitrosamine permeability constants.

CHAPTER 1: INTRODUCTION

The occurrence of *N*-nitrosamines in drinking water sources is an emerging public health issue because many nitrosamines are probable human carcinogens [1, 2]. The U.S. Environmental Protection Agency (EPA) estimated a lifetime cancer risk of 10^{-6} from consumption of drinking water containing 0.2–20 ng/L of nitrosamines, including NDMA, NMEA, NPYR, NDEA, NDPA and NDBA [2]. The California Department of Health and Human Services established a notification level of 10 ng/L for NDMA, NDEA and NDPA [3]. Concerns have been aggravated as nitrosamines, particularly NDMA, have been detected in groundwater, treated wastewater and drinking water at ng/L and μg/L levels [4-9].

Prior studies have indicated that NDMA found in water supplies is likely generated through treatment processes, particularly disinfection involving chlorination and chloramination [10-12]. The formation of other nitrosamines as disinfection by-products (DBPs), although not yet examined as thoroughly as NDMA, is also possible [9, 13-15]. In addition, there is a credible concern that elevation of nitrosamine concentrations may occur within water distribution systems after prolonged contact time between nitrosamine precursors, such as dimethylamine (DMA), and residual disinfectants [6, 9, 16].

Extensive research has been conducted on NDMA removal by means of physicochemical treatment options, such as adsorption on activated carbon (AC), hydrolysis, metal complexation, ozonation and, particularly, UV photolysis [5, 17-22]. Among these techniques, adsorption on granular actuated carbon (GAC) and UV photolysis were reported to be most effective in removing or degrading NDMA. However, GAC adsorption may be faced with challenges such as competitive adsorption by natural organic matter and the cost

for adsorbents. Challenges with UV photolysis may include the formation of undesirable compounds as by-products and the regeneration of NDMA after chlorinating the UV-treated water [23], since UV photolysis generates nitrite ion (NO_2^-) and DMA, a potential precursor of NDMA.

Nanofiltration (NF) and reverse osmosis (RO) membrane processes are emerging technologies that can be used as alternative treatment processes for the removal of relatively low-molecular-weight organic contaminants from surface water and wastewater [24-31]. However, few studies have been reported on nitrosamine removal by these membrane processes. The objective of this study was to quantitatively evaluate the rejections and transport behaviors of selected nitrosamines through commonly used high-pressure membranes. The target nitrosamines included NDMA, NMEA, NPYR, NDEA, NDPA, NDBA and NDPHA. Cross-flow filtration experiments were performed to assess the effects of operating parameters such as pressure and feed concentration of target contaminants.

CHAPTER 2: LITERATURE REVIEW

2.1. Removal of Organic Pollutants by NF and RO Membranes

Membrane processes have been chosen to achieve high removals of water/wastewater constituents, such as dissolved solids, organic carbon, and inorganic ions [27, 32]. However, a wide range of rejections by NF and RO membranes have been reported for certain organic compounds, such as endocrine disrupting chemicals (EDCs), pharmaceutically active compounds (PhACs), pesticides and disinfection by-products (DBPs) [24-31]. It has been demonstrated that rejections of organic compounds are influenced by the physicochemical properties of a compound (e.g., molecular size, charge, polarity, hydrophobicity, solubility and diffusivity), membrane characteristics (e.g., pore size, porosity, permeability, membrane thickness, charge and hydrophobicity), feed water characteristics (e.g., pH, ionic strength and the presence/absence of natural organic matter) as well as operating conditions (e.g., pressure, feed flow rate and recovery) [26, 27, 33, 34].

Studies have shown that negatively charged compounds generally have high rejections (e.g., >90%) due to electrostatic repulsion between anionic compounds and negatively charged membranes. The main rejection mechanism for anionic species has been related to be molecular size, charge of the compounds and pore size of the membranes [26, 35, 36]. On the other hand, the rejections of uncharged organic compounds were found to differ significantly (i.e., 10–90%), depending on molecular size, hydrophobicity and tested membranes [26, 32, 36], indicating the involvement of more complex mechanisms. Consequently, the factors that have the greatest influence on rejections of uncharged organic compounds by NF and RO membranes have not yet been thoroughly determined [37].

Particularly, the rejections of uncharged low-molecular-weight organic compounds, such as alkyl alcohols, alkyl phenols and trihalomethanes, have received great interest recently to elucidate rejection mechanisms and to investigate a correlation with solute physicochemical properties [32, 38, 39].

2.2. Solute Transport through NF Membranes

Many studies have indicated that the rejections of organic compounds by NF membranes can be attributed to a number of mechanisms: size exclusion (steric interaction), electrostatic interaction (charge/polarity exclusion), and adsorption on a membrane surface [35, 36, 40, 41]. Since nitrosamines are uncharged compounds, the ionic interactions between the compounds and membranes are assumed to be absent and steric exclusion and adsorptive effects are expected to dominate.

For uncharged compounds, the transport of solutes through NF membranes is thought to be governed by diffusive and convective flows. Furthermore, it is reported that there is an additional transport mechanism for compounds which adsorb on membranes: partitioning and subsequent diffusion through the membranes, which can result in lower rejection as compared to organic solutes which do not adsorb on membranes [27, 40, 42, 43]. The diffusion in a membrane polymer is accomplished by a series of successive jumps from one site to another in the direction of decreasing concentration, requiring an activation energy to overcome the energy barrier associated with breaking the bonds between the diffusing molecule and those surrounding it [40, 44].

CHAPTER 3: THEORY

3.1. Concentration Polarization Model

In a membrane separation process, the accumulation of solutes, rejected by a membrane, in a feed solution near the membrane wall decreases the permeate flux due to the reduction of the pressure-driving force. This enhanced solute concentration in a boundary layer (δ [L]) is termed as concentration polarization and results from the equilibrium between the convective transport (permeate flux due to the pressure) and diffusion (from the membrane wall to the bulk feed solution due to the concentration gradient). The solute transport in the concentration polarization layer can be represented as follows [45-47]:

$$\frac{c_w - c_p}{c_f - c_p} = \exp\left(\frac{J_v \delta}{D}\right) = \exp\left(\frac{J_v}{k}\right) \quad (1)$$

where c = solute concentration (subscripts of w, f and p refer to bulk feed solution, feed solution near the membrane wall, and permeate solution, respectively) [M/L^3]; J_v = volumetric solution flux [L/T]; δ = thickness of the boundary layer [L]; D = solute molecular diffusivity in aqueous solution [L^2/T]; k = solute mass transfer coefficient [L/T].

3.2. Solute Transport through RO Membranes

Although RO membranes are considered non-porous, there are generally imperfections (pores) inside the membranes. Spiegler and Kedem (1966) developed the non-equilibrium thermodynamic model to represent the steady-state permeation of water and solute molecules through a reverse osmosis membrane, taking into account the convective solute transport through imperfections. The following equations were derived for solution and solute fluxes across a differential element located within a membrane [47, 48].

$$J_v = -p_w\left(\frac{dP}{dx} - \sigma\frac{d\pi}{dx}\right) \tag{2}$$

$$J_s = J_v c_p = -p_s\frac{dc}{dx} + (1-\sigma)J_v c \tag{3}$$

$$p_w = \frac{K_W D_W^M V_W}{RT};\quad p_s = K_S D_S^M \tag{4a,b}$$

where J_v = volumetric solution flux [L/T]; p_w = specific hydraulic permeability [(L^3T)/M]; x = length of coordinate (originating from the feed/membrane interface and towards the permeate side) [L]; P = hydraulic pressure [M/(LT^2)]; σ = reflection/coupling coefficient (an indicator of degree of water/solute coupling or membrane imperfection, $0 \le \sigma \le 1$) [dimensionless]; π = osmotic pressure [M/(LT^2)]; J_s = gravimetric solute flux [M/(L^2T)]; p_s = local solute permeability [L^2/T]; $c = K_S \cdot c^M$ = fictitious aqueous solute concentration at equilibrium with the actual solute concentration inside the membrane phase (c^M) [M/L^3]; K_S and K_W = solute and water partition coefficients between aqueous and membrane phases, respectively [dimensionless]; D_W^M and D_S^M = water and solute molecular diffusivities in membrane phase, respectively [L^2/T]; V_W = water partial molar volume [L^3/mol]. Here, P, π and c refer to the average values in the solutions on both sides of a differential membrane element and it is assumed that the three coefficients (σ, p_w and p_s) are constant. By integrating Eq. (3) across the membrane thickness, the following equation can be derived.

$$\frac{c_p}{c_w - c_p} = \frac{1-\sigma}{\sigma}\frac{1}{1-\exp\left[-(1-\sigma)J_v/P_S\right]} \tag{5}$$

Solution and solute fluxes can also be approximated as follows [48]:

$$J_v = \frac{p_w}{\delta_m}(\Delta P - \sigma\Delta\pi) = P_W(\Delta P - \sigma\Delta\pi) \approx P_W(P_f - \sigma\pi_w + \sigma\pi_p) \tag{6}$$

$$J_s = \frac{p_s}{\delta_m}\Delta c + (1-\sigma)J_v\bar{c} = P_S\Delta c + (1-\sigma)J_v\bar{c} \tag{7}$$

$$\Delta P = P_f - P_p \approx P_f \; ; \quad \Delta\pi = \pi_w - \pi_p \quad \text{and} \quad \Delta c = c_w - c_p \tag{8a-c}$$

where δ_m = membrane thickness [L]; P_f and P_p = pressure provided in feed and pressure in permeate (≈ 1 atm), respectively [M/(LT^2)]; π_w and π_p = osmotic pressures corresponding to solute concentrations in the feed solution near the membrane wall and in the permeate, respectively [M/(LT^2)]; $P_W = p_w/\delta_m$ = hydraulic permeability [(L^{2}T)/M]; $P_S = p_s/\delta_m$ = solute permeability [L/T]; $\bar{c}$ = average solute concentration of c_w and c_p [M/L^3].

Eqs. (2) and (6) imply that solution flux is proportional to the difference between the hydraulic and osmotic pressures and osmotic pressure is affected by the reflection coefficient (σ). Eqs. (3) and (7) indicate that solute flux is a combination of solute transport by diffusion due to the concentration gradient and by convection whose extent is influenced by the coupling degree (σ) between solute and water. When there is no water/solute coupled permeation (a perfect RO membrane), σ equals unity, whereas solute transport will be governed mainly by convection when σ approaches zero.

By combining the Spiegler-Kedem model with the concentration polarization model, i.e., Eqs. (5) and (1), the following equation can be derived to determine transport parameters in conjunction with the mass transfer coefficient [33, 45, 47]:

$$\frac{c_f - c_p}{c_p} = \frac{R_0}{1 - R_0} = \frac{\sigma}{1 - \sigma} \frac{1 - \exp\left[-(1 - \sigma) J_v / P_S\right]}{\exp\left(J_v / k\right)} \tag{9}$$

where $R_0 = 1 - (c_p / c_f)$ = apparent (observed) rejection [dimensionless].

3.3. Estimation of Transport Parameters

Under the assumptions of solute permeation solely by diffusion, i.e., no water/solute coupling (σ = 1) and/or negligible concentration polarization, i.e., infinite mass transfer coefficient (k = ∞), the transport parameters (P_S, σ and/or k) can be estimated by non-linear

or linear regressions of simplified forms of Eq. (9) [47]. Alternatively, the transport parameters (σ and P_S) can be estimated by using a non-linear regression of Eq. (9), based on the experimental data of R_0 versus J_v taken at different pressures. Mass transfer coefficients (k) can be determined either by a non-linear regression simultaneously with the other two parameters [33, 45] or separately by an independent experiment [46].

3.4. Determination of Mass Transfer Coefficients

There are several methods reported to determine a mass transfer coefficient (k) [45, 46] and two of them will be examined for a comparison in this study.

A mass transfer coefficient is dependent on feed channel geometry, feed water flow regime, and solute. It can be related to feed channel configuration and feed water velocity by means of dimensionless numbers [49]:

$$k = \frac{2(Sh)(Q_f)}{(A_C)(Sc)(Re)} \tag{10}$$

where $Sh = (k \cdot h)/D$ = Sherwood number [dimensionless]; $Sc = \nu/D$ = Schmidt number [dimensionless]; $Re = (2 \cdot h \cdot Q_f)/(\nu \cdot A_C)$ = Reynolds number [dimensionless]; h = height of feed channel [L]; Q_f = feed flow rate [L^3/T]; A_C = cross-sectional area of feed channel [L^2]; ν = kinematic viscosity [L^2/T]. For plane, smooth-walled channels in laminar flow region ($Re < 10^3$), Sherwood number can be expressed with Schmidt and Reynolds numbers [50]:

$$Sh = 2.94[(h/l)Sc\,Re]^{1/3} \tag{11}$$

where l = length of a feed channel [L]. By substituting Eq. (11) into Eq. (10) for two different solutes (A and B) and correlating the resulting equations, the following equation can be obtained:

$$\frac{k_A}{k_B} = \left(\frac{D_A}{D_B}\right)^{\frac{2}{3}} \tag{12}$$

where k_A and k_B = mass transfer coefficients of species A and B, respectively [L/T]; D_A and D_B = molecular diffusivities of species A and B, respectively [L^2/T]. The equation above can be used to calculate the mass transfer coefficient of each nitrosamine (k_{NA}), using the mass transfer coefficient of salt (k_{NaCl}), molecular diffusivity of salt ($D_{NaCl} \approx 1.39 \times 10^{-5}$ [cm^2/sec], empirically estimated value for 2 g/L of NaCl at 20 ºC [51]), and molecular diffusivity of each nitrosamine (D_{NA}). The following equation can be used to estimate k_{NaCl} experimentally, based on the evaluation of the permeate flux decline induced by the addition of salt to an initially salt-free feed solution [46]:

$$k_{NaCl} = \frac{(J_v)_{SALT}}{\ln\left\{\frac{\Delta P}{\pi_f - \pi_p}\left[1 - \frac{(J_v)_{SALT}}{(J_v)_{WATER}}\right]\right\}} \tag{13}$$

where $(J_v)_{SALT}$ and $(J_v)_{WATER}$ = volumetric permeate fluxes of salt-containing and salt-free solutions, respectively [L/T]. Eq. (13) includes the assumption that the reflection coefficient of NaCl (σ_{NaCl}) is unity (i.e., only diffusion), which would be reasonable for a solute like NaCl with high rejections (>98%) by RO membranes. The molecular diffusivity of each nitrosamine can be calculated using the Wilke-Chang equation for diffusivities in dilute solutions for non-electrolytes [44] (listed as D_{NA} in Table 1):

$$D_{AB} = \frac{1.17 \times 10^{-13} (\xi_B M_B)^{1/2} T}{V_A^{0.6} \mu_B} \tag{14}$$

where D_{AB} = diffusivity of A in dilute solution of B [m^2/sec]; ξ_B = association factor of solvent B (2.6 for water); M_B = molecular weight of solvent [g/mol]; T = temperature [K]; V_A = molar volume of solute A at the normal boiling point [m^3/kmol]; μ_B = viscosity of solution

B [cP]. In the case of a single electrolyte, the osmotic pressure can be expressed as follows [47, 49]:

$$\pi = c_T RT\phi \tag{15}$$

where c_T = total concentration of ions and molecules present in a solution [mol/L]; R = ideal gas law constant = 0.08206 [L·atm/(mol·K)]; T = temperature [K]; ϕ = molar osmotic coefficient [dimensionless]. The empirical equation of the osmotic coefficients for NaCl solutions at concentrations (c) ranging from 0.0001 to 0.3 M was reported as follows [47]:

$$\log(1-\phi) = -1.09373 - 0.08101 \log c - 0.17492 (\log c)^2 - 0.01785 (\log c)^3 \tag{16}$$

Alternatively, by assuming that $\sigma = 1$ and combining Eqs. (1) and (7), the following equation can be developed to determine the mass transfer coefficients of nitrosamines. By plotting $\ln[J_v(1–R_0)/R_0]$ versus J_v, the mass transfer coefficients of nitrosamines (k_{NA}) can be obtained from the slopes of linear regressions [33, 46]:

$$\ln\left(J_v \frac{1-R_0}{R_0}\right) = \frac{J_v}{k} + \ln P_S \tag{17}$$

CHAPTER 4: MATERIALS AND METHODS

4.1. Solution Preparation

All chemicals used were of analytical-reagent grade unless otherwise stated. Deionized water, produced from a Millipore Milli-Q Nanopure water purification system, was used throughout. NDMA, NPYR, NDEA, NDPA, NDBA and NDPHA (>99%) were purchased from Sigma-Aldrich (St. Louis, MO) and NMEA (>95%) was purchased from VWR (Suwanee, GA). The relevant physicochemical properties and structures of the target nitrosamines are presented in Table 1 and Figure 1. The nitrosamines were mixed and diluted with methanol to prepare nitrosamine stock solutions with concentrations typically at 5 g/L. The deuterated forms of NDMA and NDPA, NDMA-d_6 and NDPA-d_{14}, were used as internal standards. Dichloromethane (98%, from Cambridge Isotope Laboratories, Inc., Andover, MA) containing 1 g/L of NDMA-d_6 and NDPA-d_{14} was diluted with methanol to desired concentrations in order to prepare spiking solutions, which were added into samples of water matrices for extraction recovery calculations. To prepare standard solutions (25–500 μg/L) for GC/MS analysis, the nitrosamine stock solution (in methanol) and internal standard original solutions (in dichloromethane) were mixed and diluted with dichloromethane. All solutions were securely capped and stored in amber bottles in a freezer to minimize photodegradation and evaporation.

Table 1. Physicochemical properties of target nitrosamines

Nitrosamine Compound	Molecular Formula	MW [g/mol]	Logarithm of octanol-water partitioning coefficient (Log Kow)	Aqueous Diffusivity[*1] at 20 °C (D_{NA}) [$\times 10^6$ cm^2/s]	Henry's Law Constant at 25°C [$\times 10^6$ $atm \cdot m^3/mol$]
NDMA	$C_2H_6N_2O$	74	–0.57	9.90	1.20[*2]
NMEA	$C_3H_8N_2O$	88	0.04	8.68	1.44[*3]
NPYR	$C_4H_8N_2O$	100	–0.19	8.06	0.012[*2]
NDEA	$C_4H_{10}N_2O$	102	0.48	7.79	3.63[*2]
NDPA	$C_6H_{14}N_2O$	130	1.36	6.57	2.25[*2]
NDBA	$C_8H_{18}N_2O$	158	2.63	5.75	316[*2]
NDPHA	$C_{12}H_{10}N_2O$	198	3.13	5.76	660[*4]

[*1] Calculated value using Eq. (14)
[*2] Syracuse Research Corporation CHEMFATE
[*3] ChemIDPlus TEXNET®
[*4] EPA (1982)

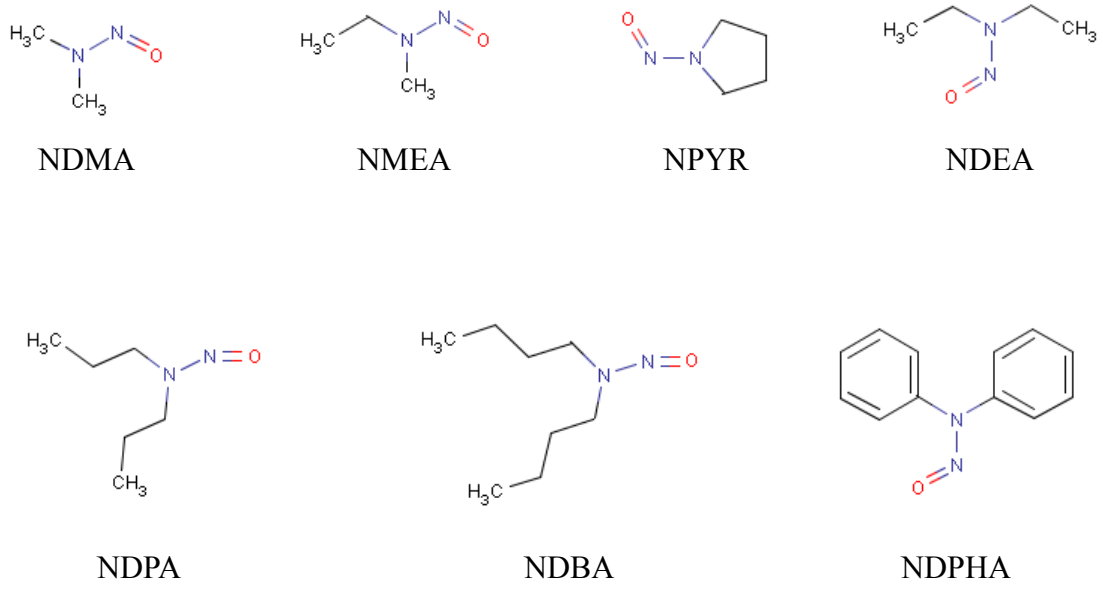

Figure 1. Structures of target nitrosamines

4.2. Analytical Methods

4.2.1. Solid-Phase Extraction (SPE)

An aliquot (10–25 μL) of the internal standard spiking solution was added to each sample (5–625 mL, stored in an amber bottle) to obtain a desired concentration of internal standards. 200 mg of Ambersorb 572 adsorbent beads (Supelco, St. Louis, MO), which were baked at 300 °C for 3 hours prior to use to minimize organic contamination, were added into the sample to extract nitrosamines. The sample containing the adsorbents was placed on a shaker at 220 rpm for 2 hours and was subsequently filtered with a glass fiber filter (Millipore, Billerica, MA) to collect the adsorbent beads. The collected adsorbents were air-dried at room temperature for 3 hours. After drying, the adsorbents were transferred to a 2 mL amber vial and 0.5 mL of dichloromethane was added into the vial to desorb nitrosamines from the adsorbent beads. The vial was immediately capped and stored in a refrigerator until GC/MS analysis. The concentration factor, the sample volume divided by the volume of dichloromethane added (0.5 mL), varied from 10 to 1250, depending on the sample volume.

4.2.2. Liquid-Liquid Extraction (LLE)

Similarly to SPE, the internal standard spiking solution was added into a sample. The same amount of dichloromethane as that of the sample (typically 3.0 mL) was added into the sample, resulting in a concentration factor of unity. The sample was then gently mixed for three minutes to enhance the interfacial mass transfer between water- and dichloromethane-phases. Approximately 1 mL of dichloromethane phase of the sample was transferred into a 2 mL amber vial. The vial was immediately capped and stored in a refrigerator until GC/MS analysis.

4.2.3. Extraction Recovery Calculation

It is crucial to obtain accurate extraction recoveries particularly when dealing with samples of low concentrations. In general, internal standards can be utilized to estimate extraction recoveries of corresponding compounds; for instance, NDMA-d_6 can accurately represent NDMA in terms of extraction behaviors. Since only two internal standards (NDMA-d_6 and NDPA-d_{14}) were used, it was essential to find a method to estimate the extraction recoveries of nitrosamines other than NDMA and NDPA.

Seven replicate samples, containing nitrosamines and internal standards, were prepared and extracted through SPE or LLE. The average values of the extraction recovery ratios of each nitrosamine to either of the two internal standards are presented in Table 2 with coefficients of variation (CV). This test confirmed that the recovery ratios determined were consistent among the seven replicates for each compound.

Each time SPE or LLE was performed, a dummy sample containing a known concentration of nitrosamines and internal standards was prepared and extracted along with actual samples. The extraction recoveries of nitrosamines in actual samples were calculated based on the recovery ratios determined from the dummy sample and the recoveries of two internal standards for actual samples. For each nitrosamine, two recoveries could be obtained on the basis of the recoveries of two internal standards. Although the difference between these two recoveries fell within 10%, the average value was used to calculate the recovery of each compound to obtain more accurate extraction recoveries.

Table 2. Average value of extraction recovery ratio of each nitrosamine to (A) NDMA-d_6 or (B) NDPA-d_{14} obtained from seven replicate samples through SPE

Compound	(A) NDMA-d_6		(B) NDPA-d_{14}	
	Average	CV [%]	Average	CV [%]
NDMA-d_6	1.00	N/A	0.88	2.10
NDPA-d_{14}	1.13	2.13	1.00	N/A
NDMA	1.01	0.68	0.89	2.31
NMEA	1.11	1.22	0.98	1.34
NPYR	1.03	2.33	0.91	0.38
NDEA	1.15	1.09	1.02	1.19
NDPA	1.13	2.00	0.99	0.82
NDBA	1.08	3.97	0.95	1.89

4.2.4. Gas Chromatography/Mass Spectrometry (GC/MS)

After either SPE or LLE, samples were analyzed using a GC/MS (Agilent 6890 GC/5973 MS) with a Supelco Equity^{TM} – 1701 column (30 m × 250 μm × 0.25 μm). Either splitless or solvent-vent injection mode (typical injection vol. of 1 and 5 μL, respectively) was used with a programmable temperature vaporization (PTV) based large volume injector (LVI) capable of a broad range of volume injection and preconcentration. Nitrosamines were identified and quantified using selected ion monitoring (SIM) mode with 74.1 m/z (parent ion) and 42 (daughter ion) for NDMA, 80.1 and 48 for NDMA-d_6, 88.1 and 56 for NMEA, 100.1 and 68 for NPYR, 102.1 and 56.1 for NDEA, 130.2 and 70 for NDPA, 144.2 and 78 for NDPA-d_{14}, 158.2 and 84 for NDBA, and 169.1 and 51 for NDPHA.

4.2.5. High Performance Liquid Chromatography (HPLC)

A 100 μL aliquot of a water sample was injected into an Agilent 1100 Series HPLC equipped with a C18 reversed phase column and a UV/VIS detector. A mobile phase of acetonitrile-water mixture (60:40) was used at a constant flow rate of 1.0 mL/min. NDPA and

NDBA were measured at wavelength of 220 nm and NDPHA was measured at a wavelength of 200 nm. The detection limit of NDPA and NDBA was 50 ppb, while the detection limit of NDPHA was 25 ppb.

4.3. Membranes

Two NF and four brackish RO membranes were selected from two manufacturers: Saehan Industries Inc. and Filmtec. NF membranes included NE70 (Saehan) and NF90 (Filmtec). All brackish RO membranes were from Saehan Industries Inc.: BE (normal), FE (fouling resistant), nFE (enhanced fouling resistant) and BLN (low-pressure). All membranes were polyamide thin-film composite but varied in salt rejection and permeate flux. The membrane specifications by manufacturers are provided in Table 3.

Table 3. Membrane specifications by manufacturers

Module		Manufacturer	Material	Salt Rejection [%]	Permeate Flux [LMH]
NF	NF90	Filmtec	Polyamide Thin Film Composite	> 97[*1]	40.5
	NE70	Saehan		99.5[*2]	38.2
RO	RE8040–BE			99.5[*3]	46.6
	RE8040–FE			99.5[*3]	46.6
	RE8040–nFE			99.5[*3]	46.6
	RE8040–BLN			99.2[*4]	50.9

[*1] 2000 ppm of $MgSO_4$ at 75 psi
[*2] 2000 ppm of $MgSO_4$ at 70 psi
[*3] 2000 ppm of NaCl at 225 psi
[*4] 1500 ppm of NaCl at 150 psi

4.4. Experimental Apparatus

The experimental apparatus consisted of four custom-designed cross-flow plate-and-frame cells: two pairs of test cells placed in parallel (Figure 2). Each test cell was equipped with lower and upper plates (stainless steel 316) with a flat sheet membrane in

between, sealed with rubber silicon rings. Permeate lines were located in the upper plates. The active membrane area was approximately 25 cm^2 and the feed channel height was 5 mm. The cross-flow velocity at a typical flow rate of 0.8 GPM (per line) was 0.3 m/sec. The feed solution in a 35 L stainless steel feed tank was circulated and both permeate and concentrate were returned to the feed tank to maintain the feed concentration constant. Pressure to the cells was controlled and measured by a needle pressure valve and an industrial pressure gauge (Swagelok, Solon, OH), located downstream of the cells. To minimize adsorption and corrosion, all the tubing and fittings were made of stainless steel 316 and Teflon®.

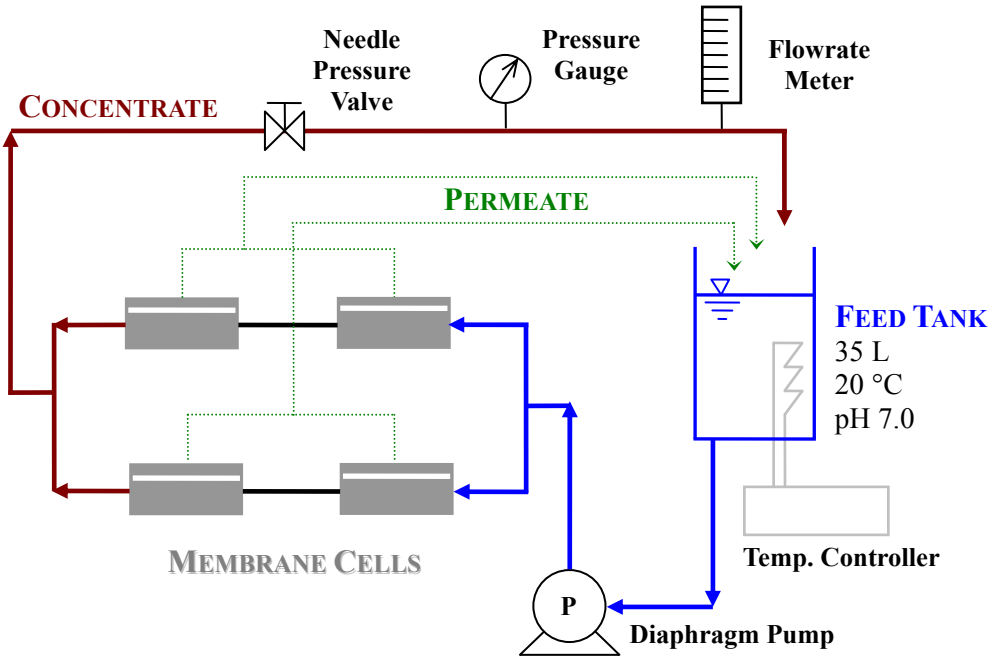

Figure 2. Schematic of a bench-scale cross-flow filtration apparatus.

4.5. Experimental Procedures

4.5.1. Nitrosamine Filtration Experiments

Membrane coupons were cut out from membrane flat sheets to match the feed channel size. They were then soaked in Milli-Q water for at least 24 hours at room temperature before installation into cells. After placing membrane coupons into cells, they were compacted at

140 psi and 450 psi, respectively for NF and RO membranes, until water flux was stabilized. Permeate fluxes were measured by a digital balance and a stop watch. To ensure membrane quality, salt rejections were tested using $MgSO_4$ and NaCl, respectively for NF and RO membranes, at feed concentrations and pressures specified by the manufacturers (Table 3). Only the membranes whose salt rejections and permeate fluxes fell within ±3% and ±10% of manufacturer specifications were used for nitrosamine filtration experiments. The experimental setup was rinsed with Milli-Q water until conductivity was less than 1 μS/cm. After adding a solution containing 1mM phosphate buffer (adjusted to pH 7.0) to the feed tank, a temperature controller (Polystat, Cole-Parmer Instrument Company, Vernon Hills, IL) and a diaphragm pump (hydra-cell, Wanner Engineering, Inc., Minneapolis, MN) with a pulsation dampener installed at the pump outlet were switched on. This allowed the experimental setup to equilibrate at a set temperature (20°C), flow rate (1.6 GPM in overall) and pressure for at least one hour before spiking nitrosamines.

4.5.2. Mass Transfer Coefficient of Sodium Chloride

Membrane filtration experiments both for water and NaCl were conducted at 5 different pressures (100, 160, 220, 280 and 340 psi) and a constant feed flow (0.8 GPM per line, corresponding to a channel Reynolds number of 207) to determine mass transfer coefficient of NaCl (k_{NaCl}). The experiments were carried out by first measuring the salt-free permeate flux, $(J_v)_{WATER}$, then adding salt to obtain a feed concentration of 2,000 mg/L and measuring the salt-containing permeate flux, $(J_v)_{SALT}$. Feed and permeate concentrations of NaCl were measured by a conductivity meter.

4.6. Estimation of Transport Parameters

A nitrosamine filtration experiment was conducted at 5 different pressures (100, 160, 220, 280 and 340 psi) to obtain corresponding apparent rejections (R_0) and permeate fluxes (J_v). Once mass transfer coefficients of nitrosamines were determined, the other transport parameters (σ and P_S) were estimated by non-linear regressions of Eq. (9) using a curve fitting tool of MATLAB® (Mathworks Inc., Natick, MA).

CHAPTER 5: RESULTS AND DISCUSSION

5.1. Analytical Errors

Analytical errors associated with extraction procedures and GC/MS analyses may lead to erroneous observations concerning experimental data. However, few studies have covered this point. To determine the errors solely related to the analytical instrument itself, coefficient of variation (CV) values from seven independent measurements of standard solutions of two concentrations (25 and 250 ppb) were evaluated, using two different GC/MS injection modes: splitless and solvent-vent modes (Table 4). With solvent-vent injection mode, the detection limit could be lowered through preconcentration by evaporating only the solvent (dichloromethane). For splitless injection mode, 1 μL of a sample was typically injected without preconcentration. At a concentration of 25 ppb, splitless mode showed much more stable signal intensity than solvent-vent mode, with CV values ranging from 1.6 to 3.9% and from 4.5 to 7.8%, respectively for splitless and solvent-vent modes, depending on nitrosamine compounds. On the other hand, at a concentration of 250 ppb, both injection modes had similar CV values with the maximum CV of 2.4 and 1.9%, respectively for splitless and solvent-vent modes. It was decided that splitless mode should be used to obtain more accurate data if sample concentrations were greater than 25 ppb.

Subsequently, to determine the errors resulting from both extraction procedures and the analytical instrument (GC/MS), CV values of seven replicates through SPE or LLE were examined, with one time measurement for each replicate (Table 5). The results clearly indicated that the errors involved with SPE were much smaller than those with LLE. This may result from dichloromethane evaporation during shaking (3 min) of LLE samples. After

this observation, SPE was selected as an extraction method. If needed, sample dilution was made before SPE so that estimated sample concentrations in dichloromethane after extraction could fall within 25−500 ppb.

Table 4. CV values obtained from seven-time measurements of two standard solutions using different injection modes: splitless and solvent-vent modes

Nitrosamine Compound	Coefficient of Variation [%]			
	25 ppb		250 ppb	
	Splitless	Solvent-vent	Splitless	Solvent-vent
NDMA	1.6	4.5	1.8	1.8
NDMA-d_6	1.8	4.5	1.7	1.8
NMEA	3.9	5.5	2.1	1.7
NPYR	3.2	6.6	2.1	1.9
NDEA	2.0	4.8	2.4	1.6
NDPA	2.4	5.6	1.8	1.4
NDPA-d_{14}	2.1	5.9	1.9	1.5
NDBA	2.2	7.8	2.1	1.7

Table 5. CV values obtained from seven replicates through SPE or LLE procedures with one-time measurement using splitless injection mode (GC/MS)

Nitrosamine Compound	Coefficient of Variation [%]	
	SPE	LLE
NDMA	2.4	6.2
NDMA-d_6	2.3	7.0
NMEA	2.5	5.7
NPYR	2.8	8.2
NDEA	2.5	6.8
NDPA	2.6	6.9
NDPA-d_{14}	2.7	7.5
NDBA	4.0	8.4

5.2. Nitrosamine Rejections by NF and RO Membranes

5.2.1. Time-Dependent Nitrosamine Rejections

The rejections of uncharged compounds, particularly hydrophobic ones, could be time dependent, primarily due to adsorption on membranes during the initial phase of filtration until membranes are saturated [26]. Therefore, time to reach steady-state rejections of nitrosamines was first evaluated by selected membranes (NF: Saehan NE70 and Filmtec NF90, RO: Saehan BE). Nitrosamine feed concentrations of 520 (±60) and 890 (±60) ppb and operating pressures of 70 and 100 psi were utilized for NF and RO filtration experiments, respectively. The elevated feed concentrations were used for ease of nitrosamine analysis, as feed concentrations would have negligible effects on nitrosamine rejections as discussed below. The temperature and pH of the system were 20.0 (±0.2) °C and 7.0 (±0.4). The permeate fluxes of NF (NE70 and NF90) and RO membranes were 37.6 (±0.8), 41.8 (±2.0) and 19.6 (±0.4) LMH.

The plots of nitrosamine rejections versus filtration time are shown in Figure 3 for the filtration experiments using NF (Saehan NE70) and RO (Saehan BE) membranes. Also, the feed and permeate concentrations from the NF and RO filtration experiments are shown in Figure A-1 and Figure A-2 in Appendix. As can be seen in Figure A-1, there was a significant decrease of NDPHA feed concentration over time (7% in 7 hours) in the NF filtration experiment. This feed concentration decrease was most likely due to evaporation, which was confirmed by the control experiment without membranes. Nitrosamine rejections reached steady state within 45 minutes for the NF and RO membranes, except for NDPHA. At the early stage of filtration (≤ 4 hrs), NDPHA permeate concentrations increased continuously as NDPHA adsorption on polyamide membranes progressed and eventually reached steady-state

when the equilibrium (partitioning) between liquid- and membrane-phases was reached. This phenomenon was observed in both NF membranes. The adsorption (or partitioning) of hydrophobic compounds to the membranes is likely driven by hydrophobic or hydrogen bonding, but the exact interactions involved are not fully understood [40]. For the other nitrosamines, the first data points of the filtration experiments showed lower permeate concentrations (i.e., higher rejections). This can be attributed to the adsorption of nitrosamines on membranes to some extent at the initial stage of filtration (≤ 45min). However, the adsorption of other nitrosamines was negligible compared to that of NDPHA.

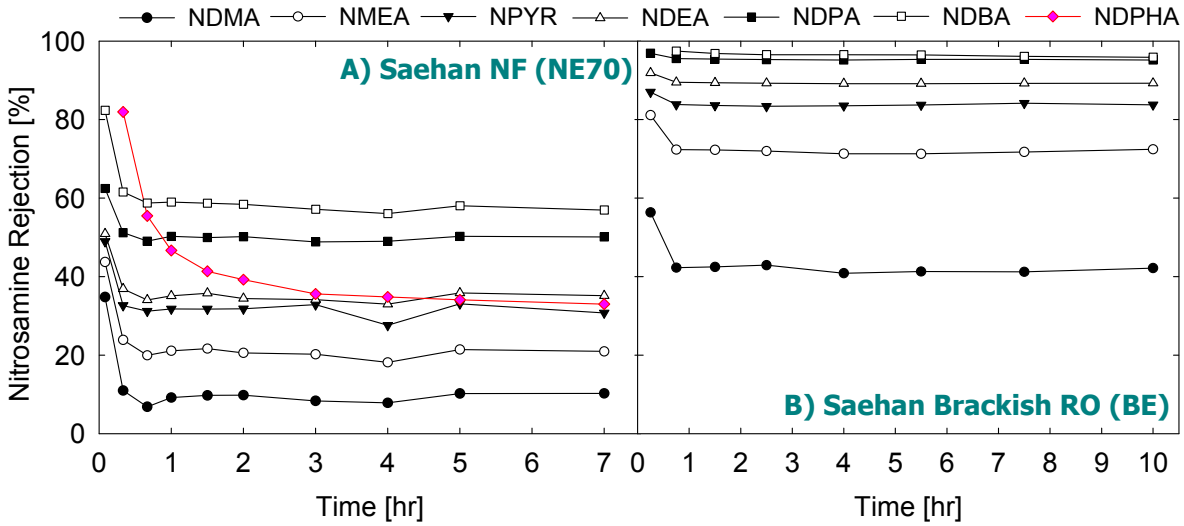

Figure 3. Nitrosamine rejections over time at pH 7.0 and 20 °C: A) NF membrane: Saehan NE70, feed concentration of 525 ppb at 70 psi; B) RO membrane: Saehan BE, 880 ppb of feed concentration at 100 psi.

5.2.2. Feed Concentration Effect on Steady-State Rejection

Analysis becomes challenging for contaminants existing at very low concentration levels in the environment. Although it has been demonstrated that there are feed concentration effects on the rejections of charged species [52-55], whether or not feed concentrations affect the membrane rejection performances of uncharged species has been controversial [26, 30]. Furthermore, few studies have conducted filtration experiments with multiple feed concentrations to examine feed concentration effects.

The feed concentration effect on steady-state rejection was examined using a representative nitrosamine compound, NDMA. A filtration experiment by a RO membrane (Saehan BE) was conducted with different NDMA feed concentrations over three orders of magnitude, ranging from 0.4 to 900 ppb. Each permeate sample was taken 1 hour after adding NDMA into the feed solution to obtain a desired feed concentration. The operating pressure and permeate flux were 220 psi and 39.7 (±1.5) LMH, respectively.

NDMA rejections ranged from 60 to 65% with tested feed concentrations. To assess the significance of these rejection differences, the extent of analytical errors was evaluated using a CV value of 2.4%, previously determined for NDMA when analyzed through SPE followed by GC/MS with splitless injection mode (Table 5). NDMA rejections are shown in Figure 4, together with the potential analytical error ranges. This result reveals that there is no statistically significant feed concentration effect on steady-state NDMA rejections. Similar results are very likely on steady-state rejections of other nitrosamine compounds.

Although the lowest feed concentration of 0.4 ppb is relatively higher than the concentration level found in the environment [4-9], it is probable that there is a similar tendency at lower concentration ranges. Thus, it was concluded that it would be reasonable to

use elevated feed concentrations for future nitrosamine filtration experiments if analytical limitations (e.g., instrumental detection limit and sampling volume) would hinder experiments.

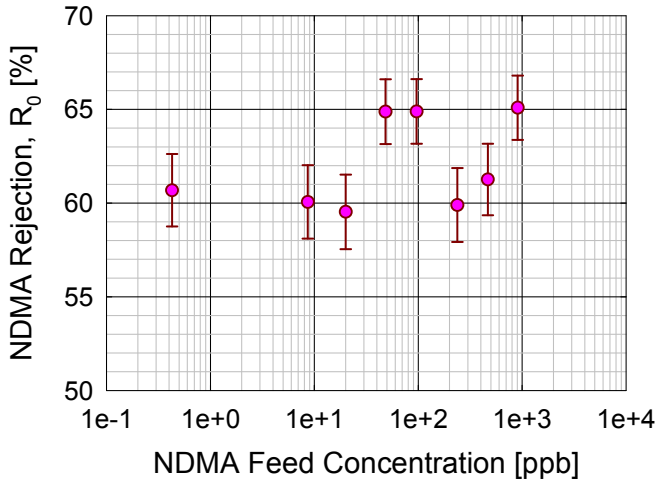

Figure 4. NDMA rejection with different NDMA feed concentrations of approximately 0.4–900 ppb at 220 psi, pH 7.0 and 20 °C by Saehan brackish RO (BE); the error range was determined using a CV value of 2.4%, previously determined for NDMA analyzed through SPE followed by GC/MS with splitless injection mode.

5.2.3. Steady-State Nitrosamine Rejection Comparison

The plots of steady-state nitrosamine rejection versus nitrosamine molecular weight are presented in Figure 5 for 2 NF membranes (Saehan NE70 and Filmtec NF90) as well as 4 RO membranes (Saehan BE, BLN, FE and nFE). The steady-state nitrosamine rejections through NF membranes varied considerably, ranging from 9 to 55% and from 15 to 75% for Saehan NE70 and Filmtec NF90, respectively. The results indicated that Saehan NE70 was a looser membrane than Filmtec NF90. The steady-state nitrosamine rejections through RO membranes also varied greatly, ranging from 54 to 97%. All of the RO membranes showed similar rejections for each nitrosamine compound, which could be expected as all of them were manufactured by the same company. Among the four RO membranes, Saehan RO (BE) consistently showed the highest rejections.

For both NF and RO membranes, there was a tendency that as molecular weight increased, nitrosamine rejections increased, with the exception of NDPHA. This trend was more explicit for relatively hydrophilic nitrosamines (Log Kow < 2). Many researchers have demonstrated that molecular weight would be an appropriate parameter for the description of rejections [35, 37, 56-58].

Partitioning has been reported to be great between polyamide active layer of thin film composite membranes and aromatic compounds (e.g., aniline, hydroquinone and benzyl alcohol) [42]. A comparable result was obtained in this study since NDPHA adsorbed considerably on membranes at the initial stage of filtration (discussed previously). These findings suggest that partitioning and subsequent diffusion of NDPHA through the membranes can occur [40], resulting in lower rejection than the expected rejection by size exclusion compared to other nitrosamines.

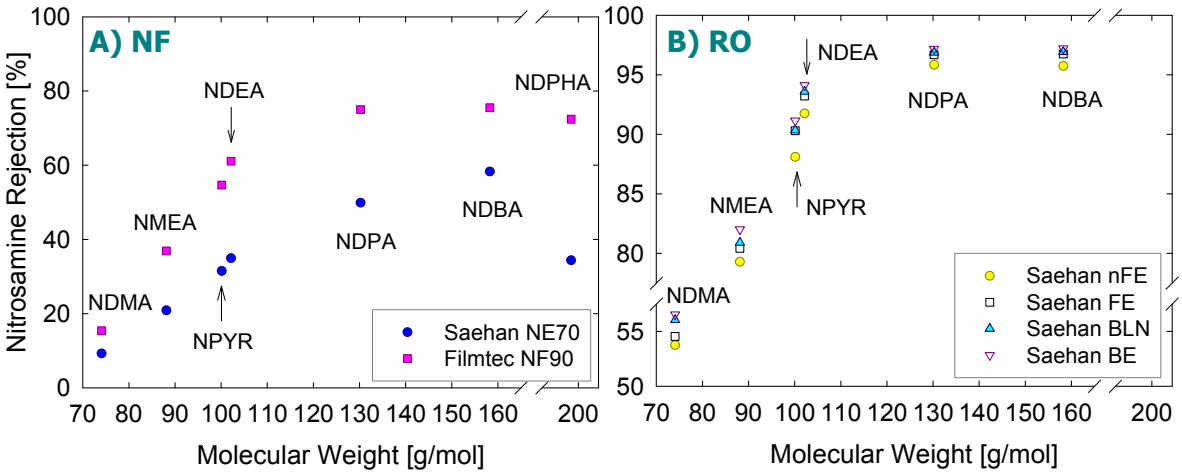

Figure 5. Steady-state nitrosamine rejection at 20 °C and pH 7.0: A) NF membranes: feed concentration of 525 (±60) ppb at 70 psi; B) RO membranes: feed concentration of 940 (±70) ppb at 220 psi.

5.3. Spiegler-Kedem Model with Concentration Polarization Model

5.3.1. Steady-State Nitrosamine Rejections at Varying Pressures

Since NF membranes showed lower nitrosamine rejections and RO membranes would be more appropriate for application to nitrosamine-contaminated water, it was decided to analyze only RO membranes according to the Spiegler-Kedem model with the concentration polarization model. A nitrosamine filtration experiment was conducted at 5 different pressures using a feed concentration of 940 (±70) ppb with 3 RO membranes (Saehan BE, FE and BLN). The steady-state nitrosamine rejections at different pressures are provided in Table A-1 in Appendix and presented as a function of pressure in Figure 6. Rejections increased as pressure increased for every nitrosamine compound and this was observed for all 3 RO membranes. This rejection increase is mainly due to a higher solution flux (J_v) obtained as pressure increased, resulting in a lower permeate concentration. This filtration experiment result was utilized to determine solute permeabilities (P_S) and reflection coefficients (σ).

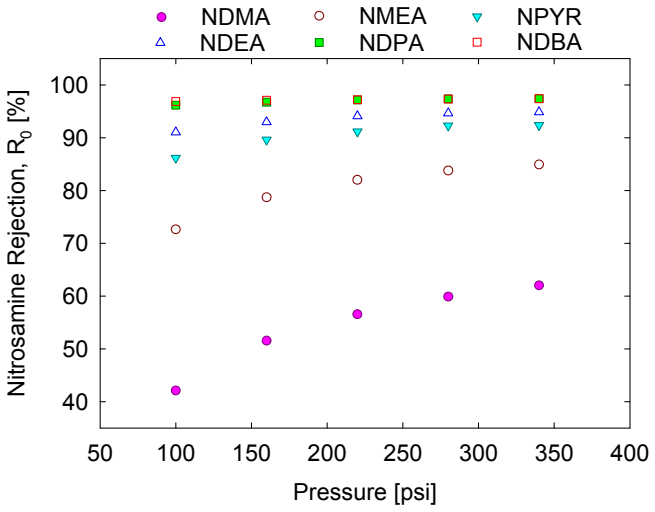

Figure 6. Steady-state nitrosamine rejections versus pressure for Saehan RO (BE) at 20 °C, pH 7.0 and feed concentration of 940 (±70) ppb.

5.3.2. Estimation of Mass Transfer, Reflection, and Solute Permeability Coefficients

As explained previously, there are various ways to estimate mass transfer coefficients but two methods were used in this study.

Using the assumption that the reflection coefficients of nitrosamines (σ_{NA}) equal unity (no solute/water coupling), the mass transfer coefficients of nitrosamines (k_{NA}) were determined by linear regressions based on Eq. (17) (correlation coefficients, $R^2 > 0.97$) and then the other transport parameters (σ and P_S) were determined by non-linear regressions according to Eq. (9) (presented in Table A-2 in Appendix). Most of the reflection coefficients exceeded unity, which is unreasonable since σ should be from 0 to 1. This probably results from the assumption made for the determination of mass transfer coefficients of nitrosamines ($\sigma_{NA} = 1$). Thus, another way to determine mass transfer coefficients of nitrosamines was explored.

The mass transfer coefficients of NaCl (k_{NaCl}) were first determined experimentally using Eq. (13) (Table A-3 in Appendix). The mass transfer coefficients of NaCl determined at 5 different pressures were relatively consistent, except for the negative values determined based on the data taken at 100 psi. By using the average values of those determined at the other 4 pressures, the mass transfer coefficients of nitrosamine (k_{NA}) were then estimated according to Eq. (12). They were used to determine the other transport parameters (σ_{NA} and P_S) by non-linear regressions according to Eq. (9). The model fit (the Spiegler-Kedem model with the concentration polarization model) with the experimental data is presented in Figure 7 and the transport parameters determined are shown in Table 6.

The experimental data fit the model very well ($R^2 > 0.94$) with the transport parameters determined by non-linear regressions, with the exception of NDBA. The low

correlation with the experimental data for NDBA was expected, because of the greater analytical errors of NDBA associated with SPE and GC/MS than those for the other nitrosamine compounds, as previously presented in Table 5.

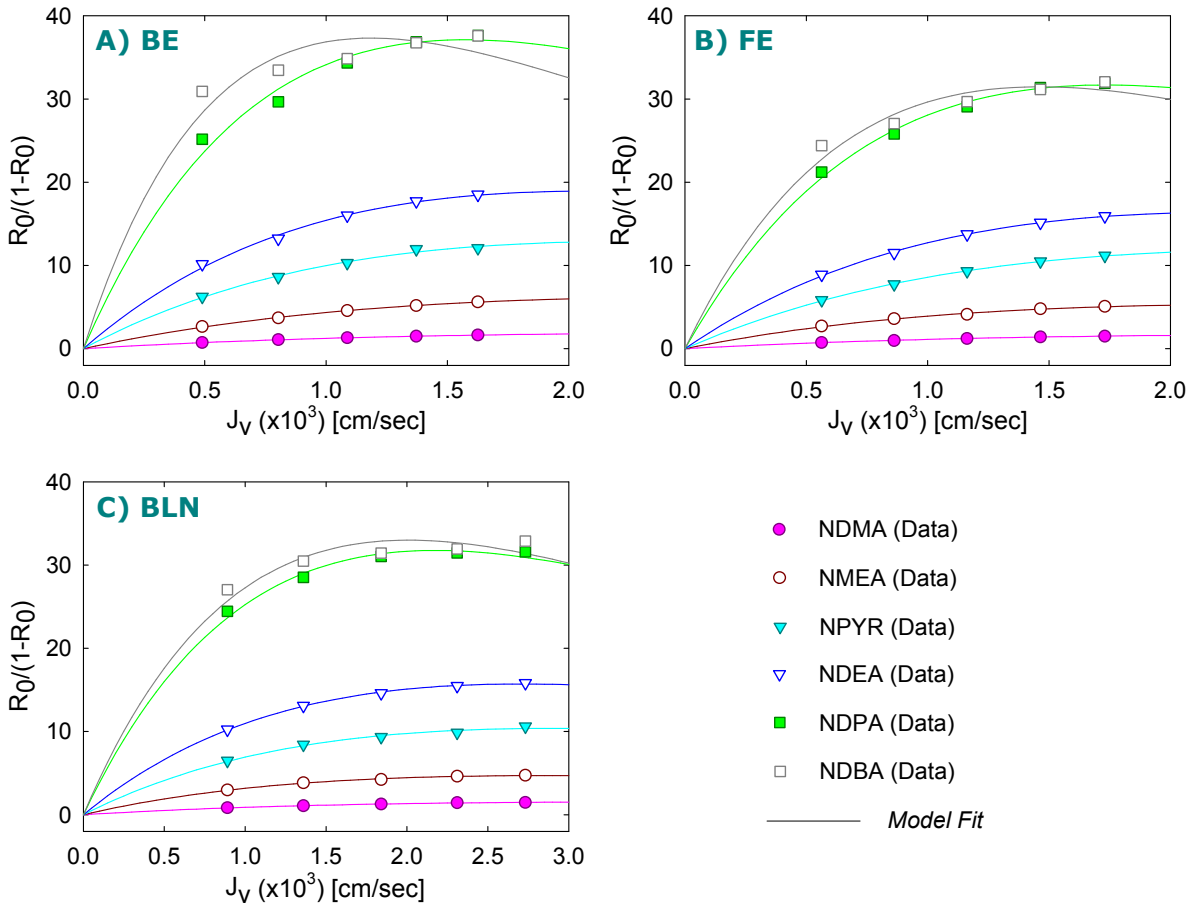

Figure 7. Spiegler-Kedem model with the experimental data of nitrosamine apparent rejections (R_0) and permeate fluxes (J_v): A) Saehan RO (BE), B) Saehan RO (FE) and C) Saehan RO (BLN).

Table 6. Transport parameters and correlation coefficients (R^2) estimated by non-linear regressions using Eq. (9): k_{NA} determined based on k_{NaCl} obtained from the independent experiment using Eq. (13)

Saehan RO Membranes	Parameters		NDMA	NMEA	NPYR	NDEA	NDPA	NDBA
BE	k_{NA}	[cm/sec]	3.41E-03	3.12E-03	2.97E-03	2.90E-03	2.59E-03	2.37E-03
	σ_{NA}	[-]	0.950	0.983	0.986	0.988	0.991	0.989
	P_S	[cm/sec]	5.47E-04	1.56E-04	6.31E-05	3.90E-05	1.49E-05	1.08E-05
	R^2	[-]	0.9998	0.9980	0.9916	0.9918	0.9439	0.3298
FE	k_{NA}	[cm/sec]	3.63E-03	3.32E-03	3.16E-03	3.09E-03	2.76E-03	2.53E-03
	σ_{NA}	[-]	0.941	0.964	0.988	0.987	0.990	0.989
	P_S	[cm/sec]	6.22E-04	1.64E-04	7.75E-05	4.94E-05	1.93E-05	1.62E-05
	R^2	[-]	0.9974	0.9920	0.9991	0.9981	0.9867	0.8438
BLN	k_{NA}	[cm/sec]	4.23E-03	3.87E-03	3.69E-03	3.60E-03	3.22E-03	2.94E-03
	σ_{NA}	[-]	0.928	0.957	0.984	0.987	0.992	0.992
	P_S	[cm/sec]	7.94E-04	2.12E-04	1.00E-04	6.17E-05	2.44E-05	2.18E-05
	R^2	[-]	0.9947	0.9940	0.9824	0.9981	0.9607	0.6630

5.3.3. Interpretation of Reflection Coefficients and Solute Permeability Coefficients

As can be seen in Table 6, as molecular weight increased, the reflection coefficients (σ_{NA}) increased (except for NDBA), indicating that nitrosamines with higher molecular weight are less likely to transport coupled with convective transport of water through possible membrane imperfections (pores). In order to compare solute permeabilities (P_S) found for different nitrosamines and RO membranes, the logarithm of solute permeability (Log P_S) was plotted against molecular weight in Figure 8 with quadratic polynomial regressions. Figure 8 reveals that solute permeabilities decreased with increasing molecular weight, indicating that larger molecules diffuse less effectively through membranes. Among the 3 RO membranes, BE had the smallest solute permeabilities and BLN showed the largest solute permeabilities.

An attempt was made to find a correlation between solute permeabilities and nitrosamine physicochemical properties (e.g., molecular weight, hydrophobicity or aqueous

diffusivity). Previous studies on the rejections of aromatic pesticides by polyamide NF membranes have shown that there is a linear or polynomial correlation between Log P_S and molecular weight or molecular width [28, 58] and a comparable tendency was found in Figure 8. Similar research has found that Log P_S is a function of molecular width and hydrophobicity (Log Kow) or the logarithm of partitioning coefficient between aqueous- and membrane-phase concentrations (Log K_S) [59]. Moreover, prior research on the rejections of cationic and anionic ions by polyamide RO membranes has demonstrated that there is a linear correlation between Log P_S and aqueous diffusivity [60]. As presented in Figure 9, a linear correlation between Log P_S and aqueous diffusivity was found ($R^2 > 0.95$). Furthermore, a strong correlation was observed between solute permeability (P_S) and molecular weight if exponential regression was used (Figure 10).

However, the regressions used both in this study and literatures were not based on any mechanistic models. Back to the Spiegler-Kedem model, solute permeability (P_S) is a function of partitioning coefficient (K_S) and diffusivity in membrane phase (D_S^M). Thus, it would be difficult to elucidate the precise correlation between solute permeability and physicochemical properties of a compound, unless the correlations between parameters such as K_S and D_S^M and physicochemical properties of a compound are clearly determined.

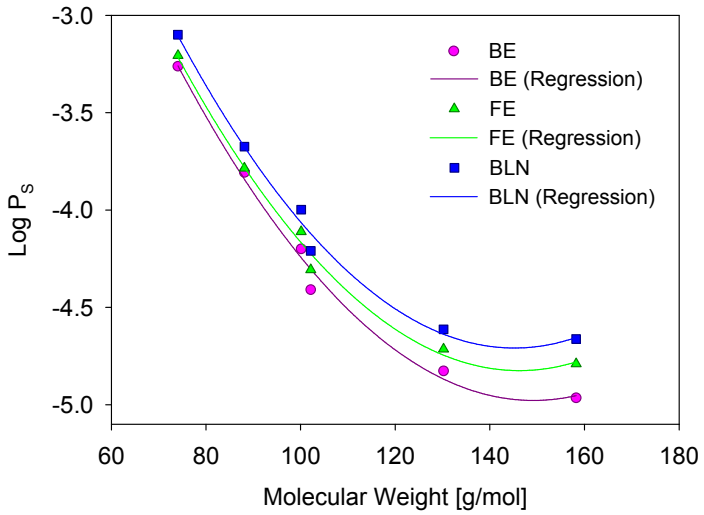

Figure 8. Correlation between the logarithm of solute permeability (Log P_S) and molecular weight for 3 Saehan RO membranes (quadratic polynomial regression).

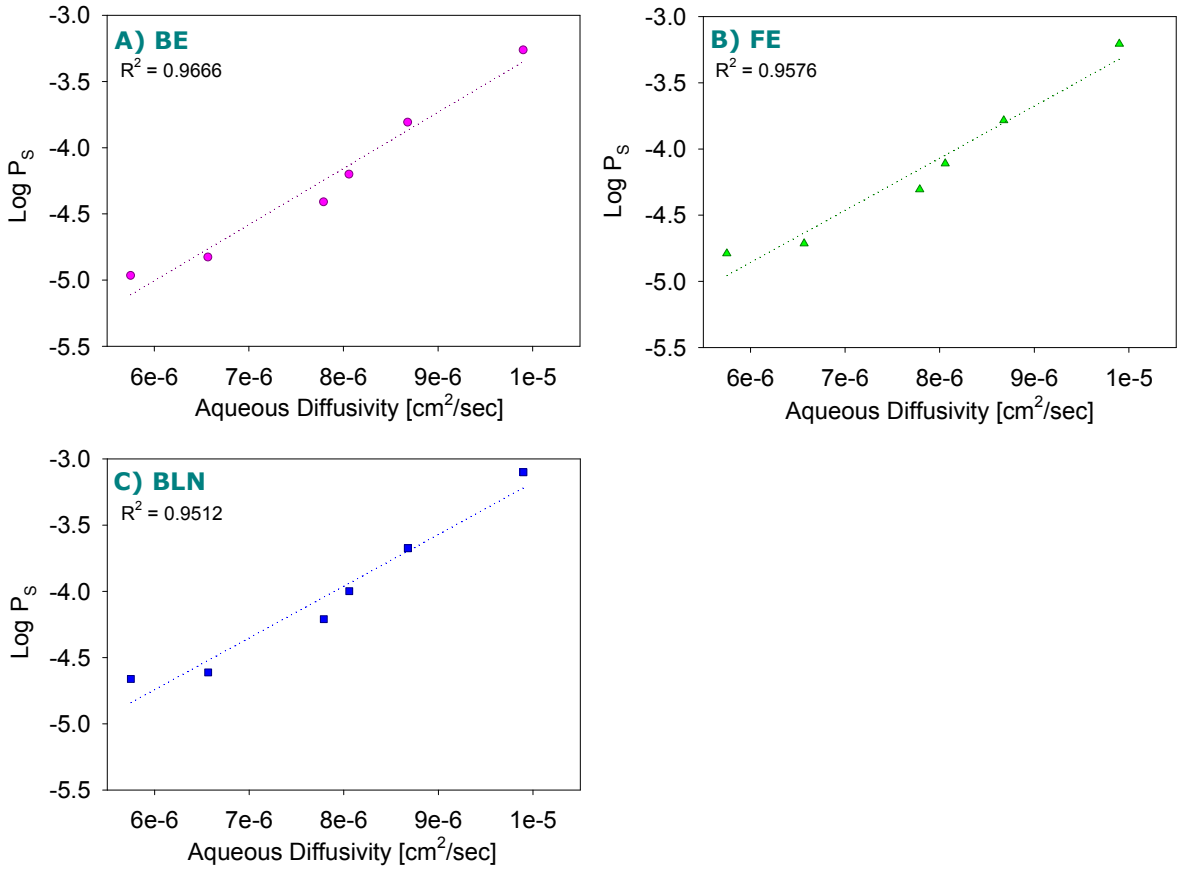

Figure 9. Linear correlation between the logarithm of solute permeability (Log P_S) and aqueous diffusivity (regression) for 3 Saehan RO membranes.

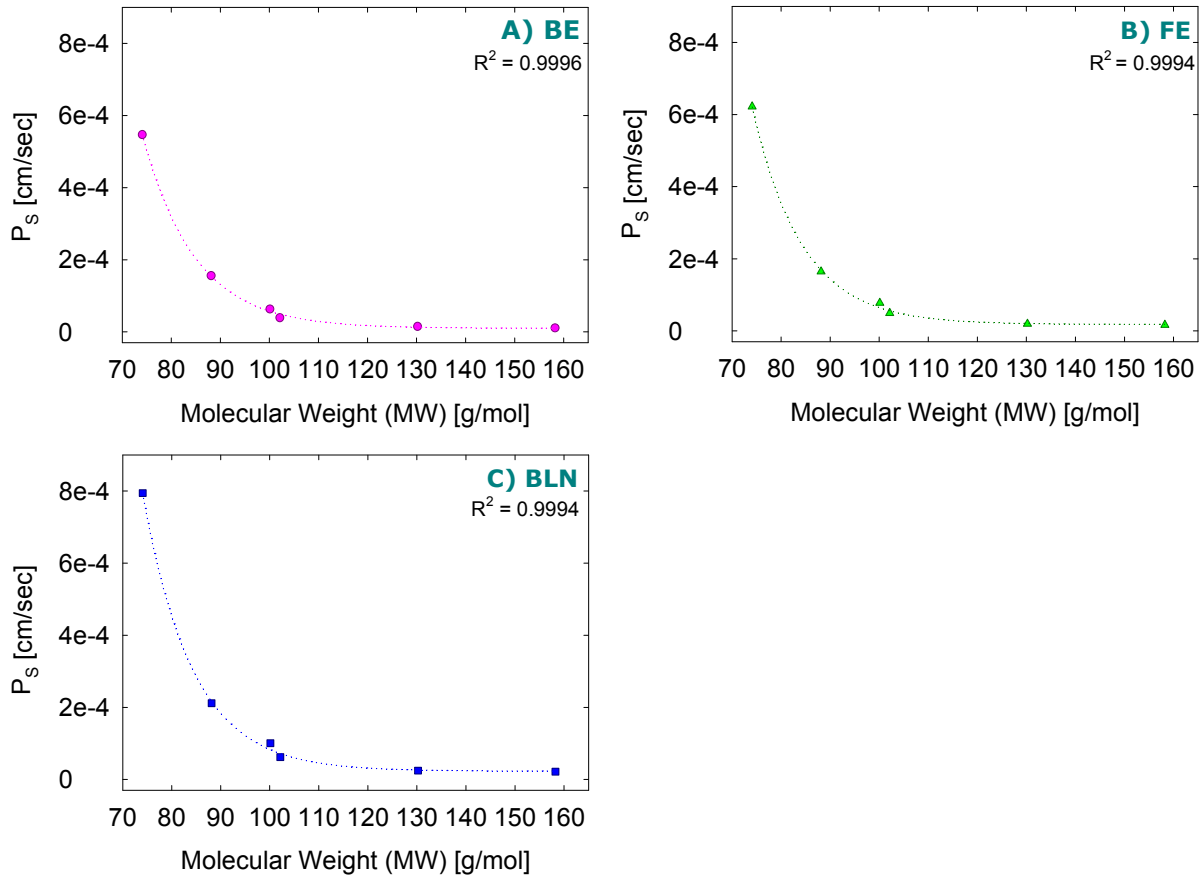

Figure 10. Correlation between solute permeability (P_S) and molecular weight (exponential regression) for 3 Saehan RO membranes.

5.3.4. Contributions of Diffusion and Convection to Solute Flux

As represented in Eq (3), there are diffusion and convection contributions to solute flux. To further understand the nature of solute transport inside the membrane, the contribution of each transport mechanism (diffusion and convection) can be approximated according to Eq. (7). The nitrosamine feed concentration adjacent to a membrane wall (c_w) was first estimated from experimental data (J_v, c_f, and c_p) and mass transfer coefficient (k_{NA}) using Eq. (1). It was found that solute wall concentrations increased to approximately twice as high as the bulk feed concentrations at higher pressures. The solute fluxes calculated are

presented in Table A-4 in Appendix. Solution and solute fluxes (J_v and J_s) increased with increasing pressure. The increase of solute flux (J_s) at higher pressure is accounted for by more enhanced wall concentration (c_w) due to the accumulation of rejected solutes associated with higher solution flux (J_v).

The percentage contributions by diffusion and convection were calculated for each nitrosamine and at each pressure (Table 7 and Table 8). Table 7 shows that the permeation of lower molecular weight nitrosamines such as NDMA, NMEA and NPYR was mainly due to diffusion (>80%). This accounts for the low levels of rejections of these compounds. In comparison, the contribution of diffusion to solute transport for higher molecular weight nitrosamines went down to approximately 50%.

The percentage contributions of diffusion are shown in Figure 11 as a function of pressure for a Saehan RO (BE) membrane. This reveals that the contribution of diffusion (or convection) is strongly dependent on pressure. As pressure (or solution flux J_v) increased, the permeation by diffusion contributed less to solute flux, i.e., permeation by convection contributed more to solute flux. The other RO membranes (FE and BLN) also showed the same tendency. Subsequently, the average values among different pressures were used to find a correlation between the contribution of diffusion and molecular weight (Figure 12). Although data are scattered, it can be said that the permeation by diffusion contributed less to solute flux for nitrosamines with higher molecular weight such as NPYR, NDEA, NDPA and NDBA.

Table 7. Percentage contribution of diffusion to solute flux for 3 RO membranes

Membrane	Pressure [psi]	Contribution of **Diffusion** to Solute Flux [%]					
		NDMA	NMEA	NPYR	NDEA	NDPA	NDBA
BE	340	88.5	90.5	83.1	78.7	67.0	53.0
	280	89.4	91.6	85.2	81.3	70.5	57.1
	220	90.5	93.0	87.7	84.4	75.0	62.6
	160	91.6	94.3	90.3	87.7	80.1	69.2
	100	93.0	95.9	93.4	91.8	86.7	78.5
FE	340	87.0	81.1	86.6	80.4	69.0	61.9
	280	88.1	83.1	88.3	82.7	72.4	65.6
	220	89.2	85.4	90.3	85.6	76.6	70.5
	160	90.3	88.1	92.3	88.6	81.4	76.1
	100	91.8	90.9	94.5	91.9	86.8	82.8
BLN	340	82.5	75.0	80.8	77.2	67.7	66.6
	280	84.1	77.6	83.0	79.9	71.2	70.1
	220	85.6	80.7	85.8	83.1	75.5	74.6
	160	87.3	84.2	88.8	86.7	80.5	79.8
	100	89.4	87.9	91.9	90.5	86.1	85.6

Table 8. Percentage contribution of convection to solute flux for 3 RO membranes

Membrane	Pressure [psi]	Contribution of **Convection** to Solute Flux [%]					
		NDMA	NMEA	NPYR	NDEA	NDPA	NDBA
BE	340	11.5	9.5	16.9	21.3	33.0	47.0
	280	10.6	8.4	14.8	18.7	29.5	42.9
	220	9.5	7.0	12.3	15.6	25.0	37.4
	160	8.4	5.7	9.7	12.3	19.9	30.8
	100	7.0	4.1	6.6	8.2	13.3	21.5
FE	340	13.0	18.9	13.4	19.6	31.0	38.1
	280	11.9	16.9	11.7	17.3	27.6	34.4
	220	10.8	14.6	9.7	14.4	23.4	29.5
	160	9.7	11.9	7.7	11.4	18.6	23.9
	100	8.2	9.1	5.5	8.1	13.2	17.2
BLN	340	17.5	25.0	19.2	22.8	32.3	33.4
	280	15.9	22.4	17.0	20.1	28.8	29.9
	220	14.4	19.3	14.2	16.9	24.5	25.4
	160	12.7	15.8	11.2	13.3	19.5	20.2
	100	10.6	12.1	8.1	9.5	13.9	14.4

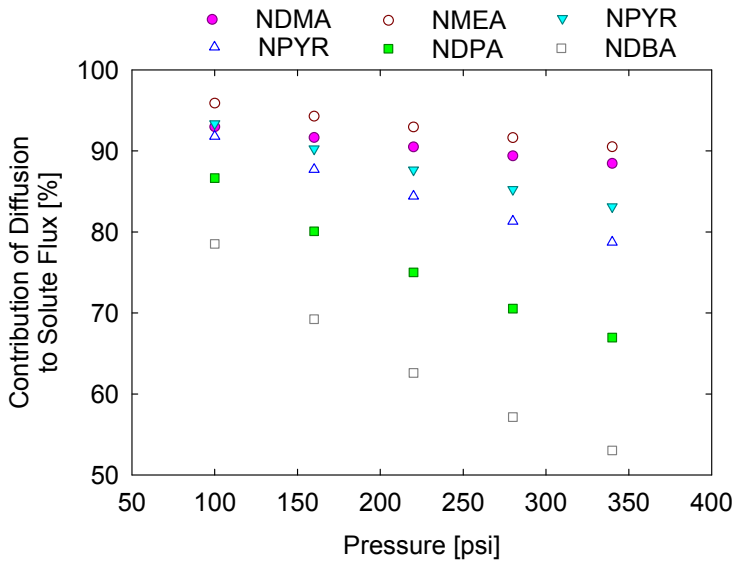

Figure 11. Percentage contribution of diffusion to solute flux for a Saehan RO membrane (BE) as a function of pressure.

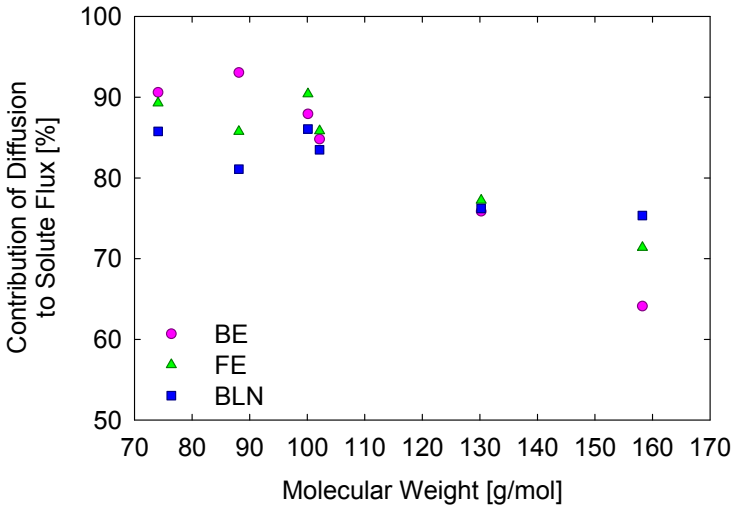

Figure 12. Percentage contribution of diffusion (average value) to solute flux versus molecular weight for 3 RO membranes.

5.3.5. Hydraulic Permeability Coefficients

According to Eq. (6), a hydraulic permeability (P_W) of a membrane can be estimated using a salt-free (pure water) or a salt-containing flux (J_w or J_v): by the slope of the plot either of J_w versus P_f based on a water permeation experiment or J_v versus ($P_f - \pi_w + \pi_p$) based on a solute permeation experiment (e.g., NaCl). The hydraulic permeabilities determined by both methods will be compared.

Water and NaCl permeation experiments were performed at 5 different pressures. Hydraulic permeabilities were estimated by plotting pure water flux (J_w) against pressure (P_f) (Table 9). Furthermore, an effort was made to estimate hydraulic permeabilities based on NaCl permeation experiments. NaCl feed concentration adjacent to a membrane wall (c_w) was first estimated and the corresponding osmotic pressures to wall and permeate concentrations (π_w and π_p) were subsequently calculated using Eqs. (15) and (16). Assuming that NaCl permeation took place solely by diffusion ($\sigma_{NaCl} = 1$), hydraulic permeabilities were then determined by linear regressions and the results are shown in Table 9 and Figure 13. There are deviations of the regression lines from the origin, i.e., the presence of a negative x-intercept (≈ 0.7 atm or 10 psi), which can be due to the un-calibrated pressure gauge used.

Hydraulic permeability should be consistent for each membrane, because it is an intrinsic value. As revealed by Table 9, the hydraulic permeabilities determined by the two methods were very similar with the difference of 0.8–1.6%, which indicates that the mass transfer coefficients of NaCl were previously determined correctly. The low-pressure RO membrane (BLN) showed the largest value of hydraulic permeability, i.e., the largest amount of pure water can go through at a specific pressure. This capacity is important for a full-scale application, because this leads to lower cost.

Table 9. Hydraulic permeabilities estimated based on pure water and solute (NaCl) permeation experiments

Saehan RO Membranes	Hydraulic Permeability (P_W) [L/(m^2·hr·bar)]		Difference [%]
	Based on J_w	Based on J_v	
BE	2.74	2.72	0.93
FE	3.04	3.02	0.82
BLN	3.65	3.59	1.57

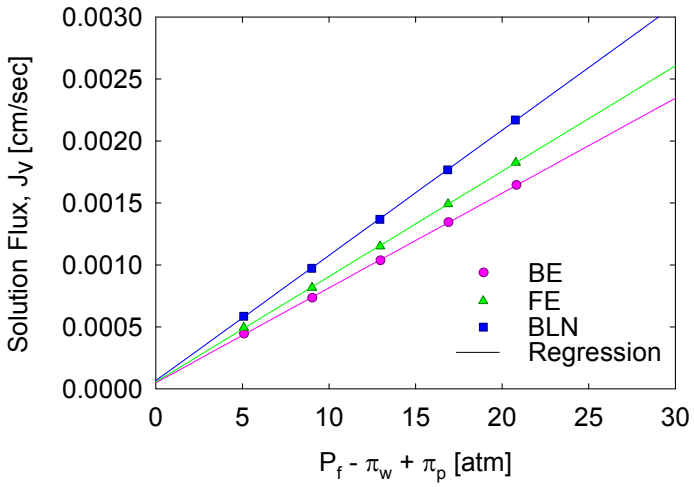

Figure 13. Linear regressions to estimate hydraulic permeabilities of 3 Saehan RO membranes based on the NaCl filtration experiment at varying pressures.

CHAPTER 6: CONCLUSION

Nitrosamine rejections by NF and brackish RO membranes varied greatly (9–75% for NF membranes and 54–97% for RO membranes) and there was a clear tendency that rejections increased with increasing molecular weight, particularly for hydrophilic compounds. For lower molecular weight nitrosamines, such as NDMA and NMEA, the solute permeation was primarily due to diffusion and this accounts for the observation that only 54–82% rejections were achieved by RO membranes. Seawater RO membranes may be able to achieve higher rejections for these lower molecular weight nitrosamines. Since nitrosamine concentrations found in water sources and drinking water are in ng/L level and the rejections of higher molecular weight nitrosamines (e.g., NDEA and NDPA) were over 90%, the brackish RO membrane process can satisfy the need to alleviate human heath concerns. The low rejection levels for NF membranes, however, indicate that they would not be appropriate for treating nitrosamine-contaminated water.

There is no statistically significant feed concentration effect on steady-state NDMA rejections. This reveals the possibility to use elevated feed concentrations than those found in the environment for filtration experiments of uncharged, relatively hydrophilic, compounds. This would significantly facilitate filtration experiments of these compounds.

To prevent possible nitrosamine formations during disinfection processes and within water distribution systems, investigation on the removal of nitrosamine precursors, such as dimethylamine (DMA), through NF/RO membranes is of great importance in future research.

APPENDIX

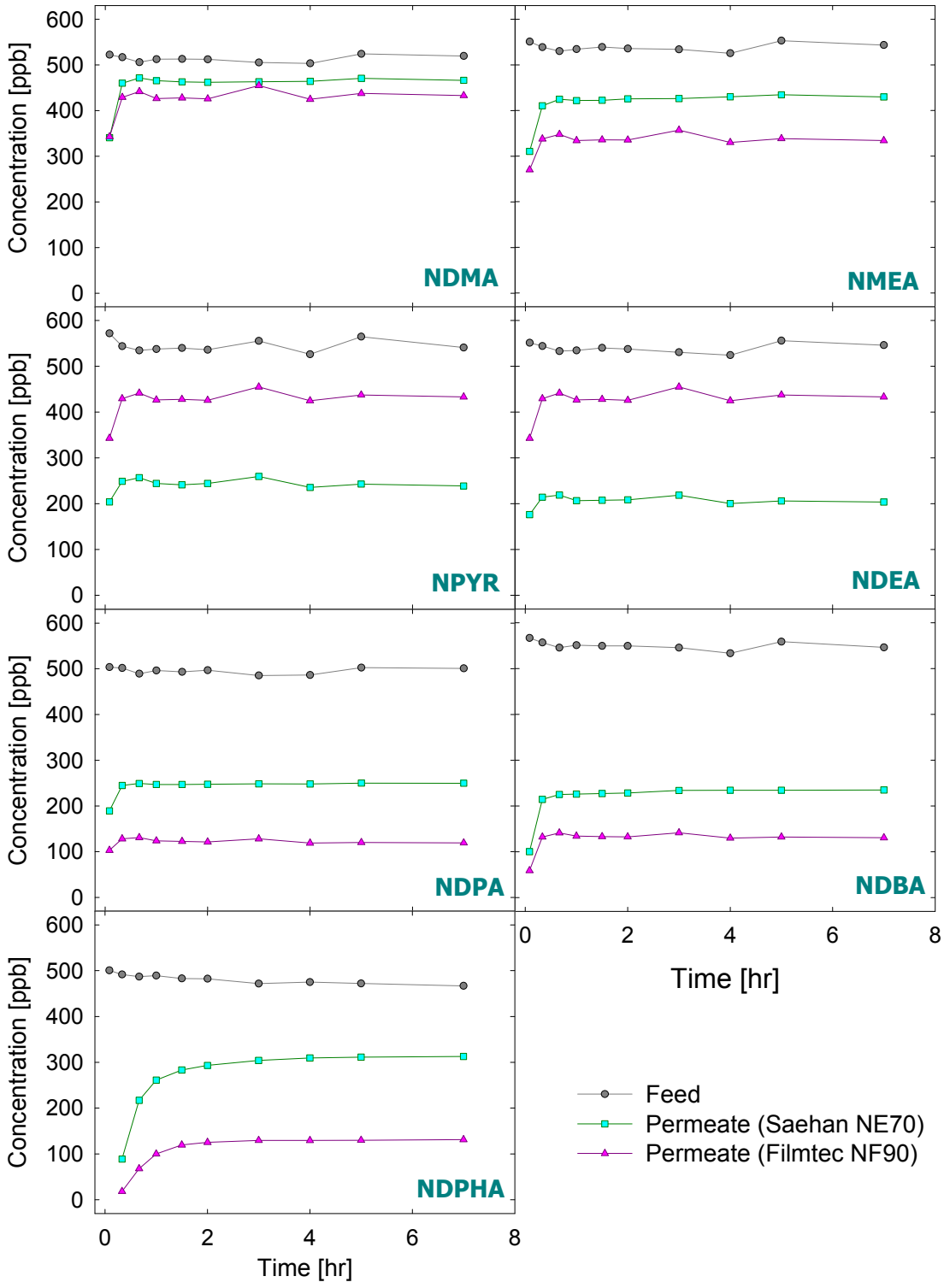

Figure A-1. Nitrosamine concentrations in feed and permeates over time through two NF membranes at 20 °C and pH 7.0.

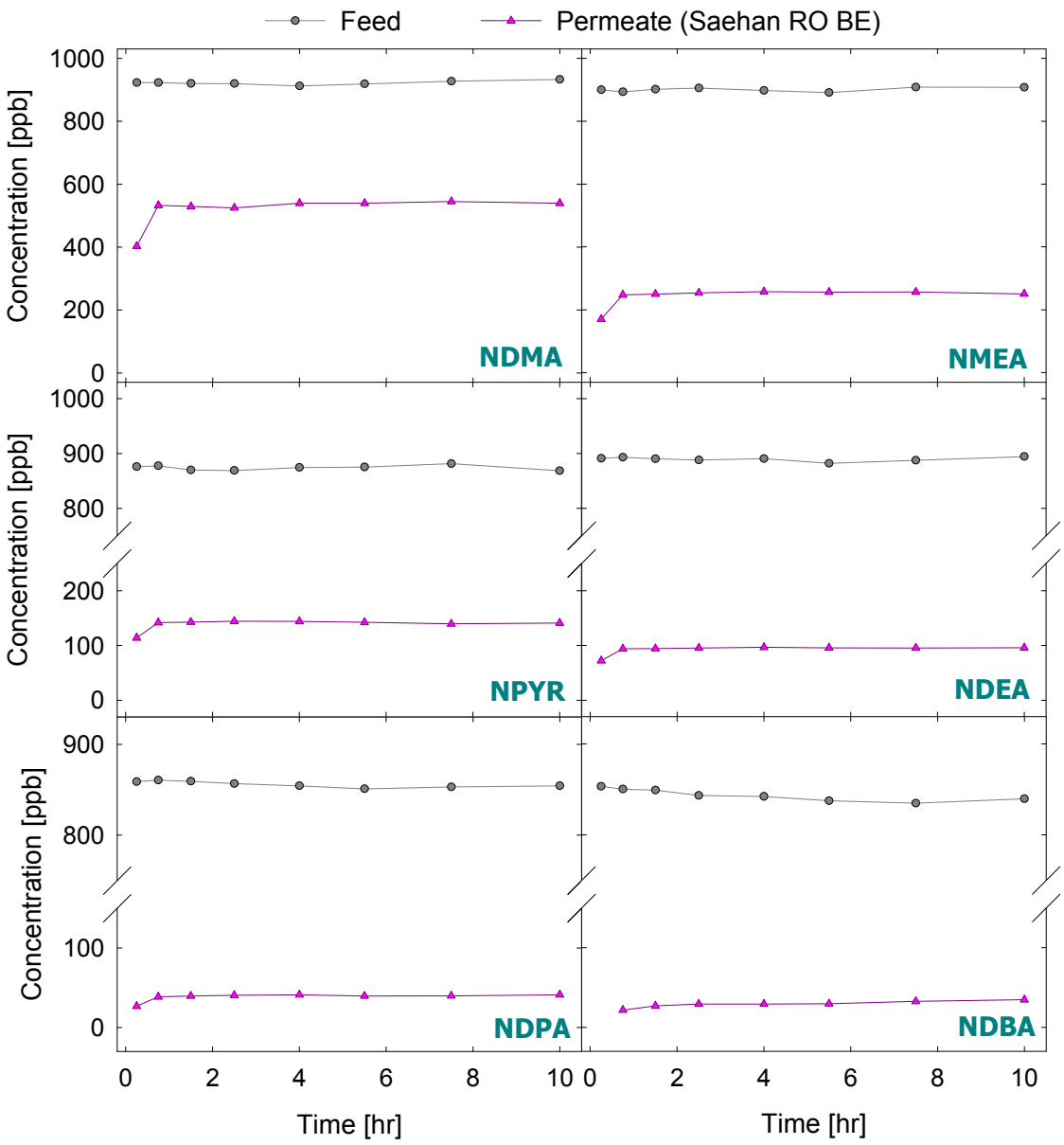

Figure A-2. Nitrosamine concentrations in feed and permeate over time through a RO membrane at 20 °C and pH 7.0.

Table A-1. Steady-state nitrosamine rejections at 5 different pressures for 3 Saehan RO membranes

Saehan RO Membranes	Pressure [psi]	NDMA	NMEA	NPYR	NDEA	NDPA	NDBA
BE	340	0.620	0.849	0.924	0.949	0.974	0.974
	280	0.599	0.838	0.923	0.947	0.974	0.974
	220	0.565	0.820	0.911	0.941	0.972	0.972
	160	0.515	0.787	0.896	0.930	0.967	0.971
	100	0.421	0.726	0.862	0.910	0.962	0.969
FE	340	0.599	0.835	0.918	0.941	0.970	0.970
	280	0.584	0.827	0.913	0.938	0.969	0.969
	220	0.545	0.804	0.903	0.932	0.967	0.967
	160	0.493	0.782	0.886	0.920	0.963	0.964
	100	0.421	0.730	0.854	0.899	0.955	0.961
BLN	340	0.596	0.826	0.914	0.941	0.969	0.970
	280	0.589	0.822	0.908	0.939	0.969	0.970
	220	0.561	0.809	0.903	0.936	0.969	0.969
	160	0.515	0.793	0.894	0.929	0.966	0.968
	100	0.454	0.748	0.866	0.911	0.961	0.964

Table A-2. Transport parameters and correlation coefficients (R^2) estimated by non-linear regressions using Eq. (9): k_{NA} determined by linear regressions using Eq. (17) under the assumption that $\sigma_{NA} = 1$

Saehan RO Membranes	Parameters		NDMA	NMEA	NPYR	NDEA	NDPA	NDBA
BE	k_{NA}	[cm/sec]	2.91E-03	2.58E-03	2.22E-03	1.96E-03	1.48E-03	1.15E-03
	σ_{NA}	[-]	1.006	1.008	1.001	1.001	1.001	1.001
	P_S	[cm/sec]	5.79E-04	1.62E-04	6.42E-05	3.97E-05	1.54E-05	1.17E-05
	R^2	[-]	0.9997	0.9971	0.9916	0.9915	0.9392	0.1952
FE	k_{NA}	[cm/sec]	3.04E-03	2.28E-03	2.49E-03	2.19E-03	1.66E-03	1.40E-03
	σ_{NA}	[-]	1.010	1.008	1.001	1.001	1.001	1.001
	P_S	[cm/sec]	6.68E-04	1.68E-04	7.88E-05	5.03E-05	1.98E-05	1.69E-05
	R^2	[-]	0.9974	0.9960	0.9990	0.9978	0.9847	0.8233
BLN	k_{NA}	[cm/sec]	3.50E-03	2.81E-03	2.84E-03	2.67E-03	2.14E-03	1.98E-03
	σ_{NA}	[-]	1.009	1.003	1.001	1.001	1.000	0.999
	P_S	[cm/sec]	8.65E-04	2.29E-04	1.03E-04	6.28E-05	2.50E-05	2.11E-05
	R^2	[-]	0.9947	0.9860	0.9819	0.9981	0.9540	0.6906

Table A-3. Mass transfer coefficients of NaCl (k_{NaCl}) for 3 RO membranes

Pressure [psi]	Mass Transfer Coefficient of NaCl, k_{NaCl} [cm/sec]		
	Saehan RO (FE)	Saehan RO (BE)	Saehan RO (BLN)
340	4.05E-03	3.73E-03	4.60E-03
280	4.11E-03	4.10E-03	4.46E-03
220	4.47E-03	4.27E-03	5.25E-03
160	5.55E-03	4.95E-03	6.87E-03
100	−7.92E-03	−5.21E-03	−7.02E-03
Average*	**4.54E-03**	**4.26E-03**	**5.30E-03**

* Average k_{NaCl} value excluding the value determined at 100 psi

Table A-4. Solute fluxes by diffusion and convection for a Saehan RO (BLN) membrane

(A) Diffusion

Pressure [psi]	Solution Flux (J_v) [cm/sec]	Solute Flux (J_s) by **Diffusion** [g/(cm^2·sec)]					
		NDMA	NMEA	NPYR	NDEA	NDPA	NDBA
340	2.73E-03	0.857	0.339	0.182	0.117	0.052	0.047
280	2.31E-03	0.766	0.302	0.162	0.104	0.046	0.041
220	1.84E-03	0.653	0.264	0.142	0.091	0.040	0.035
160	1.36E-03	0.535	0.228	0.123	0.079	0.034	0.030
100	8.90E-04	0.422	0.191	0.105	0.068	0.029	0.025

(B) Convection

Pressure [psi]	Solution Flux (J_v) [cm/sec]	Solute Flux (J_s) by **Convection** [g/(cm^2·sec)]					
		NDMA	NMEA	NPYR	NDEA	NDPA	NDBA
340	2.73E-03	0.182	0.113	0.043	0.035	0.025	0.024
280	2.31E-03	0.145	0.087	0.033	0.026	0.019	0.017
220	1.84E-03	0.110	0.063	0.023	0.018	0.013	0.012
160	1.36E-03	0.078	0.043	0.016	0.012	0.008	0.007
100	8.90E-04	0.050	0.026	0.009	0.007	0.005	0.004

REFERENCES

1. National Toxicology Program (NTP), Department of Health and Human Services, 11th Report on Carcinogens, http://ntp-server.niehs.nih.gov/index.cfm?objectid=32BA9724-F1F6-975E-7FCE50709CB4C932 (Accessed Jan 2007).

2. US Environmental Protection Agency, Integrated Risk Information System (IRIS), N-Nitrosodimethylamine, http://www.epa.gov/iris/subst/0045.htm (Accessed Jan 2007).

3. California Department of Health Services (CDHS), California Drinking Water: Activities Related to NDMA and other nitrosamines, http://www.dhs.ca.gov/ps/ddwem/chemicals/ndma/default.htm (Accessed Jan 2007).

4. California Department of Health Services (CDHS), A Brief History of NDMA Findings in Drinking Water Supplies and Related Activities, http://www.dhs.ca.gov/ps/ddwem/chemicals/NDMA/history/default.htm (Accessed Jan 2007).

5. Fleming, E. C.; Pennington, J. C.; Wachob, B. G.; Howe, R. A.; Hill, D. O., Removal of N-nitrosodimethylamine from waters using physical-chemical techniques. *Journal of Hazardous Materials* **1996,** *51*, (1-3), 151-164.

6. Zhao, Y. Y.; Boyd, J.; Hrudey, S. E.; Li, X. F., Characterization of New Nitrosamines in Drinking Water Using Liquid Chromatography Tandem Mass Spectrometry. *Environ. Sci. Technol.* **2006,** *40*, (24), 7636-7641.

7. California Department of Health Services (CDHS), Studies on the Occurrence of NDMA in Drinking Water, http://www.dhs.ca.gov/ps/ddwem/chemicals/NDMA/studies/default.htm (Accessed Jan 2007).

8. Mitch, W. A.; Sedlak, D. L., Factors controlling nitrosamine formation during wastewater chlorination. *Water Supply* **2002,** *2*, (3), 191-198.

9. Charrois, J. W. A.; Arend, M. W.; Froese, K. L.; Hrudey, S. E., Detecting N-Nitrosamines in Drinking Water at Nanogram per Liter Levels Using Ammonia Positive Chemical Ionization. *Environ. Sci. Technol.* **2004,** *38*, (18), 4835-4841.

10. Choi, J.; Valentine, R. L., Formation of N-nitrosodimethylamine (NDMA) from reaction of monochloramine: a new disinfection by-product. *Water Research* **2002,** *36*, (4), 817-824.

11. Mitch, W. A.; Sedlak, D. L., Formation of N-Nitrosodimethylamine (NDMA) from Dimethylamine during Chlorination. *Environ. Sci. Technol.* **2002,** *36*, (4), 588-595.

12. Mitch, W. A.; Sedlak, D. L., Characterization and Fate of N-Nitrosodimethylamine Precursors in Municipal Wastewater Treatment Plants. *Environ. Sci. Technol.* **2004,** *38*, (5), 1445-1454.

13. Kimoto, W. I.; Dooley, C. J.; Carre, J.; Fiddler, W., Nitrosamines in tap water after concentration by a carbonaceous adsorbent. *Water Research* **1981,** *15*, (9), 1099-1106.

14. Andrzejewski, P.; Kasprzyk-Hordern, B.; Nawrocki, J., The hazard of N-nitrosodimethylamine (NDMA) formation during water disinfection with strong oxidants. *Desalination* **2005,** *176*, (1-3), 37-45.

15. Mitch, W. A.; Sedlak, D. L., Factors controlling nitrosamine formation during wastewater chlorination. *Water Supply* **2002,** *2*, (3), 191-198.

16. Mitch, W. A.; Sharp, J. O.; Trussell, R. R.; Valentine, R. L.; Alvarez-Cohen, L.; Sedlak, D. L., N-Nitrosodimethylamine (NDMA) as a Drinking Water Contaminant: A Review. *Environmental Engineering Science* **2003,** *20*, (5), 389-404.

17. Hoigne, J.; Bader, H., Rate constants of reactions of ozone with organic and inorganic compounds in water II : Dissociating organic compounds. *Water Research* **1983,** *17*, (2), 185-194.

18. Sharpless, C. M.; Linden, K. G., Experimental and Model Comparisons of Low- and Medium-Pressure Hg Lamps for the Direct and H_2O_2 Assisted UV Photodegradation of *N*-Nitrosodimethylamine in Simulated Drinking Water. *Environ. Sci. Technol.* **2003,** *37*, (9), 1933-1940.

19. Lee, C.; Choi, W.; Kim, Y. G.; Yoon, J., UV Photolytic Mechanism of *N*-Nitrosodimethylamine in Water: Dual Pathways to Methylamine versus Dimethylamine. *Environ. Sci. Technol.* **2005,** *39*, (7), 2101-2106.

20. Lee, J.; Choi, W.; Yoon, J., Photocatalytic Degradation of *N*-Nitrosodimethylamine: Mechanism, Product Distribution, and TiO_2 Surface Modification. *Environ. Sci. Technol.* **2005,** *39*, (17), 6800-6807.

21. Gunnison, D.; Zappi, M. E.; Teeter, C.; Pennington, J. C.; Bajpai, R., Attenuation mechanisms of N-nitrosodimethylamine at an operating intercept and treat groundwater remediation system. *Journal of Hazardous Materials* **2000,** *73*, (2), 179-197.

22. Kommineni, S.; Ela, W. P.; Arnold, R. G.; Huling, S. G.; Hester, B. J.; Betterton, E. A., NDMA treatment by sequential GAC adsorption and fenton-driven destruction. *Environmental Engineering Science* **2003,** *20*, (4), 361-373.

23. Liang, S.; Min, J. H.; Davis, M. K.; Green, J. F.; Remer, D. S., Use of pulsed-UV processes to destroy NDMA *Journal of American Water Works Association* **2003,** *95*, (9), 121-131.

24. Kim, T.-U.; Amy, G.; Drewes, J. E., Rejection of trace organic compounds by high-pressure

membranes. *Water Science & Technology* **2005,** *51*, (6), 335-344.

25. Hofman, J. A. M. H.; Beerendonk, E. F.; Folmer, H. C.; Kruithof, J. C., Removal of pesticides and other micropollutants with cellulose-acetate, polyamide and ultra-low pressure reverse osmosis membranes. *Desalination* **1997,** *113*, (2-3), 209-214.

26. Kimura, K.; Amy, G.; Drewes, J. E.; Heberer, T.; Kim, T.-U.; Watanabe, Y., Rejection of organic micropollutants (disinfection by-products, endocrine disrupting compounds, and pharmaceutically active compounds) by NF/RO membranes. *Journal of Membrane Science* **2003,** *227*, (1-2), 113-121.

27. Bellona, C.; Drewes, J. E.; Xu, P.; Amy, G., Factors affecting the rejection of organic solutes during NF/RO treatment - a literature review. *Water Research* **2004,** *38*, (12), 2795-2809.

28. Jung, Y.-J.; Kiso, Y.; Rabi Atul Adawih binti, O.; Ikeda, A.; Nishimura, K.; Min, K.-S.; Kumano, A.; Ariji, A., Rejection properties of aromatic pesticides with a hollow-fiber NF membrane. *Desalination* **2005,** *180*, (1-3), 63-71.

29. Berg, P.; Hagmeyer, G.; Gimbel, R., Removal of pesticides and other micropollutants by nanofiltration. *Desalination* **1997,** *113*, (2-3), 205-208.

30. Van der Bruggen, B.; Schaep, J.; Maes, W.; Wilms, D.; Vandecasteele, C., Nanofiltration as a treatment method for the removal of pesticides from ground waters. *Desalination* **1998,** *117*, (1-3), 139-147.

31. Thanuttamavong, M.; Yamamoto, K.; Ik Oh, J.; Ho Choo, K.; June Choi, S., Rejection characteristics of organic and inorganic pollutants by ultra low-pressure nanofiltration of surface water for drinking water treatment. *Desalination* **2002,** *145*, (1-3), 257-264.

32. Yoon, Y.; Lueptow, R. M., Removal of organic contaminants by RO and NF membranes. *Journal of Membrane Science* **2005,** *261*, (1-2), 76-86.

33. Murthy, Z. V. P.; Gupta, S. K., Sodium cyanide separation and parameter estimation for reverse osmosis thin film composite polyamide membrane. *Journal of Membrane Science* **1999,** *154*, (1), 89-103.

34. Bruggen, B. V. d.; Verliefde, A.; Braeken, L.; Cornelissen, E. R.; Moons, K.; Verberk, J. Q. J. C.; Dijk, H. J. C. v.; Amy, G., Assessment of a semi-quantitative method for estimation of the rejection of organic compounds in aqueous solution in nanofiltration. *Journal of Chemical Technology & Biotechnology* **2006,** *81*, (7), 1166-1176.

35. Van der Bruggen, B.; Schaep, J.; Wilms, D.; Vandecasteele, C., Influence of molecular size, polarity and charge on the retention of organic molecules by nanofiltration. *Journal of Membrane Science* **1999,** *156*, (1), 29-41.

36. Lee, S.; Lueptow, R. M., Membrane Rejection of Nitrogen Compounds. *Environ. Sci. Technol.*

2001, *35*, (14), 3008-3018.

37. Kimura, K.; Toshima, S.; Amy, G.; Watanabe, Y., Rejection of neutral endocrine disrupting compounds (EDCs) and pharmaceutical active compounds (PhACs) by RO membranes. *Journal of Membrane Science* **2004,** *245*, (1-2), 71-78.

38. Schutte, C. F., The rejection of specific organic compounds by reverse osmosis membranes. *Desalination* **2003,** *158*, (1-3), 285-294.

39. Agenson, K. O.; Oh, J.-I.; Urase, T., Retention of a wide variety of organic pollutants by different nanofiltration/reverse osmosis membranes: controlling parameters of process. *Journal of Membrane Science* **2003,** *225*, (1-2), 91-103.

40. Nghiem, L. D.; Schafer, A. I.; Elimelech, M., Removal of Natural Hormones by Nanofiltration Membranes: Measurement, Modeling, and Mechanisms. *Environ. Sci. Technol.* **2004,** *38*, (6), 1888-1896.

41. Bowen, W. R.; Mohammad, A. W.; Hilal, N., Characterisation of nanofiltration membranes for predictive purposes - use of salts, uncharged solutes and atomic force microscopy. *Journal of Membrane Science* **1997,** *126*, (1), 91-105.

42. Ben-David, A.; Bason, S.; Jopp, J.; Oren, Y.; Freger, V., Partitioning of organic solutes between water and polyamide layer of RO and NF membranes: Correlation to rejection. *Journal of Membrane Science* **2006,** *281*, (1-2), 480-490.

43. Ben-David, A.; Oren, Y.; Freger, V., Thermodynamic Factors in Partitioning and Rejection of Organic Compounds by Polyamide Composite Membranes. *Environ. Sci. Technol.* **2006,** *40*, (22), 7023-7028.

44. Hines, A. L.; Maddox, R. N., *Mass Transfer, Fundamentals and Applications*, Pearson Education: New Jersey, 1985.

45. Murthy, Z. V. P.; Gupta, S. K., Estimation of mass transfer coefficient using a combined nonlinear membrane transport and film theory model. *Desalination* **1997,** *109*, (1), 39-49.

46. Sutzkover, I.; Hasson, D.; Semiat, R., Simple technique for measuring the concentration polarization level in a reverse osmosis system. *Desalination* **2000,** *131*, (1-3), 117-127.

47. Urama, R. I.; Marinas, B. J., Mechanistic interpretation of solute permeation through a fully aromatic polyamide reverse osmosis membrane. *Journal of Membrane Science* **1997,** *123*, (2), 267-280.

48. Spiegler, K. S.; Kedem, O., Thermodynamics of hyperfiltration (reverse osmosis): criteria for efficient membranes. *Desalination* **1966,** *1*, (4), 311-326.

49. Mariñas, B. J.; Urama, R. I., Modeling Concentration-Polarization in Reverse Osmosis Spiral-Wound Elements. *Journal of Environmental Engineering* **1996,** *122*, (4), 292-298.

50. Isaacson, M. S.; Sonin, A. A., Sherwood Number and Friction Factor Correlations for Electrodialysis Systems, with Application to Process Optimization. *Ind. Eng. Chem. Proc. Des. Dev.* **1976,** *15*, (2), 313-321.

51. Lobo, V. M. M.; Quaresma, J. L., *Physical Science Data 41, Handbook of electrolyte solutions Part B*, Elsevier: New York, 1989.

52. Garba, Y.; Taha, S.; Cabon, J.; Dorange, G., Modeling of cadmium salts rejection through a nanofiltration membrane: relationships between solute concentration and transport parameters. *Journal of Membrane Science* **2003,** *211*, (1), 51-58.

53. Ong, S. L.; Zhou, W.; Song, L.; Ng, W. J., Evaluation of feed concentration effects on salt/ion transport through RO/NF membranes with the Nernst-Planck-Donnan model. *Environmental Engineering Science* **2002,** *19*, (6), 429-439.

54. Wu, M.; Delai Sun, D.; Hwa Tay, J., Effect of operating variables on rejection of indium using nanofiltration membranes. *Journal of Membrane Science* **2004,** *240*, (1-2), 105-111.

55. Senthilmurugan, S.; Gupta, S. K., Separation of inorganic and organic compounds by using a radial flow hollow-fiber reverse osmosis module. *Desalination* **2006,** *196*, (1-3), 221-236.

56. Chen, S.-S.; Taylor, J. S.; Mulford, L. A.; Norris, C. D., Influences of molecular weight, molecular size, flux, and recovery for aromatic pesticide removal by nanofiltration membranes. *Desalination* **2004,** *160*, (2), 103-111.

57. Ozaki, H.; Li, H., Rejection of organic compounds by ultra-low pressure reverse osmosis membrane. *Water Research* **2002,** *36*, (1), 123-130.

58. Kiso, Y.; Mizuno, A.; Othman, R. A. A. b.; Jung, Y.-J.; Kumano, A.; Ariji, A., Rejection properties of pesticides with a hollow fiber NF membrane (HNF-1). *Desalination* **2002,** *143*, (2), 147-157.

59. Kiso, Y.; Sugiura, Y.; Kitao, T.; Nishimura, K., Effects of hydrophobicity and molecular size on rejection of aromatic pesticides with nanofiltration membranes. *Journal of Membrane Science* **2001,** *192*, (1-2), 1-10.

60. Masahide Taniguchi, S. K., Estimation of transport parameters of RO membranes for seawater desalination. *AIChE Journal* **2000,** *46*, (10), 1967-1973.